



UNIVERSIDAD DE INVESTIGACIÓN DE TECNOLOGÍA EXPERIMENTAL YACHAY

Escuela de Ciencias Biológicas e Ingeniería

**TÍTULO: Fatigue detection in the vastus lateralis muscle
based on sEMG signal analysis.**

Trabajo de integración curricular presentado como requisito para la
obtención del título de Ingeniera Biomedica

Autor:

Marilyn Elizabeth Figueroa Guayllas

Tutor:

Diego Alfonso Almeida Galarraga, PhD.

Urcuquí, Abril de 2024

Autoría

Yo, **Marilyn Elizabeth Figueroa Guayllas**, con cédula de identidad 0706820248, declaro que las ideas, juicios, valoraciones, interpretaciones, consultas bibliográficas, definiciones y conceptualizaciones expuestas en el presente trabajo; así cómo, los procedimientos y herramientas utilizadas en la investigación, son de absoluta responsabilidad de la autora del trabajo de integración curricular. Así mismo, me acojo a los reglamentos internos de la Universidad de Investigación de Tecnología Experimental Yachay.

Urcuquí, Abril de 2024.

Marilyn Elizabeth Figueroa Guayllas
CI:0706820248

Autorización de publicación

Yo, **Marilyn Elizabeth Figueroa Guayllas**, con cédula de identidad 0706820248, cedo a la Universidad de Investigación de Tecnología Experimental Yachay, los derechos de publicación de la presente obra, sin que deba haber un reconocimiento económico por este concepto. Además, autorizo a la Secretaría de Educación Superior, Ciencia, Tecnología e Innovación, para la publicación del presente trabajo de titulación sin fines comerciales. Declaro además que el texto del presente trabajo de titulación no podrá ser cedido a ninguna empresa editorial para su publicación u otros fines, sin contar previamente con la autorización escrita de la Universidad.

Asimismo, autorizo a la Universidad que realice la digitalización y publicación de este trabajo de integración curricular en el repositorio virtual, de conformidad a lo dispuesto en el Art. 144 de la Ley Orgánica de Educación

Urcuquí, Abril de 2024.

Marilyn Elizabeth Figueroa Guayllas
CI:0706820248

Dedication

I want to dedicate this work mainly to God and my family.

To my mother, Enny Guayllas, and my father, Fredy Figueroa, for always supporting me and encouraging me to move forward, for making me feel loved at all times, and for trusting that I can achieve everything I set my mind to.

To my brothers, Paúl Figueroa and Saúl Figueroa, for being an inspiration, for supporting me unconditionally, for their advice, and for giving me joy in my life.

To my boyfriend, Christopher Almachi, for being present in every step, supporting me in difficult moments and motivating me to improve daily.

To my friend Elizabeth Macas, whom I also thank for all her love and for being my right hand, my friend since the first day of college, my confidant.

Also, to all my friends and professors throughout my college life for making the college experience a pleasant memory full of experiences and learning that I will always carry in my heart.

Last but not least, I dedicate it to myself for all the effort year after year I put into achieving this goal of my life.

Marilyn Elizabeth Figueroa Guayllas

Acknowledgment

Thanks to my thesis director, Diego Almeida, Ph.D., for his support, time, guidance, and for encouraging me to finish my work and my student stage in the best way.

Thanks to Felix Vladimir Bonilla Venegas, Ph.D., for guiding me in the experimental stage of my work and for patiently sharing his knowledge with me.

Thanks to professor Jonathan Cruz for always being open to resolving doubts about some aspects throughout the development of my work.

Thanks to professors Kevin Landazuri and Fernando Villalba, for their observations and recommendations to my work, which allowed me to achieve a better work.

Thanks to the “Secretaria de Educación Superior, Ciencia, Tecnología e Innovación” as a sponsoring entity, on the occasion of the scholarship component “carrera elegible-2018”.

Thanks to all the Yachay Tech students who participated in my research experiments and to the professors of the sports area for opening space for me in the University gymnasium. Their collaboration was essential to develop this work.

Thanks to my brothers, Paúl and Saúl, for their unconditional support throughout my life, and to my boyfriend, Chris, for his support throughout my career.

Finally, thanks to Yachay Tech University for the learning and experiences.

Marilyn Elizabeth Figueroa Guayllas

Resumen

La electromiografía (EMG) capta las señales eléctricas producidas por la contracción de los músculos esqueléticos. El análisis de la electromiografía de superficie (sEMG) es el principal método para identificar el agotamiento muscular. La identificación de la fatiga permite crear técnicas de apoyo, y ayuda tanto a la rehabilitación clínica como a la prevención de lesiones, ya que el agotamiento muscular aumenta el riesgo de lesiones deportivas. Por ello, el presente trabajo tiene como objetivo principal el análisis de las señales sEMG en el músculo vasto lateral para la detección de la fatiga muscular después de la realización de actividades físicas que involucre a las extremidades inferiores. Con este fin, se aplicó la Transformada Wavelet a las señales sEMG adquiridas antes y después de ejercicios de gimnasio. El estudio utiliza un amplificador de señales sEMG, una tarjeta NI USB 6212 y la plataforma MATLAB para la adquisición, procesamiento y análisis de señales. La descomposición de las señales mediante la transformada wavelet con la función base biortogonal 3.5 y un 4to nivel de descomposición, permitió analizar las variaciones en la actividad muscular y caracterizarlas a través del cálculo de los parámetros valor medio absoluto (MAV), valor cuadrático medio (RMS), y frecuencia media (MNF) de las señales sEMG, mejorando así la capacidad de identificar patrones asociados con la fatiga muscular. Finalmente, se concluyó que la amplitud de los parámetros de las señales sEMG en dominio del tiempo aumenta y de los parámetros en el dominio de la frecuencia disminuyen en el estado de fatiga.

Palabras Clave:

Señales electromiográficas, sEMG, transformada wavelet, función base Bio 3/5, extracción de características, valor medio absoluto, raíz cuadrada media, frecuencia media.

Abstract

Electromyography (EMG) captures the electrical signals produced by skeletal muscle contraction. Surface electromyography (sEMG) analysis is the main method for identifying muscle exhaustion. Identifying fatigue allows for the creation of supportive techniques and aids in both clinical rehabilitation and injury prevention, as muscle exhaustion increases the risk of sports injuries. Therefore, the main objective of the present work is the analysis of sEMG signals in the vastus lateralis muscle for the detection of muscle fatigue after physical activities involving the inferior extremities. For this purpose, the Wavelet Transform was applied to the sEMG signals acquired before and after gymnastic exercises. The study uses a sEMG signal amplifier, an NI USB 6212 card, and the MATLAB platform for signal acquisition, processing, and analysis. The decomposition of the signals using the wavelet transform with the biorthogonal basis function 3.5 and a 4th level of decomposition made it possible to analyze the variations in muscle activity and characterize them through the calculation of the parameters mean absolute value (MAV), root mean square value (RMS), and mean frequency (MNF) of the sEMG signals, improving the ability to identify patterns associated with muscle fatigue. Finally, it was concluded that the amplitude of the parameters of the sEMG signals in the time domain increases and the parameters in the frequency domain decrease in the fatigue state.

Keywords:

Electromyographic signals, sEMG, wavelet transform, Bio 3/5 basis function, feature extraction, mean absolute value, mean square root, mean frequency.

Contents

Dedication	v
Acknowledgment	vii
Resumen	ix
Abstract	xi
Contents	xiii
List of Tables	xv
List of Figures	xvii
1 Introduction	1
1.1 Fatigue detection by using sEMG	1
1.2 Problem statement	2
1.3 Justification	3
1.4 Objectives	3
1.4.1 General Objective	3
1.4.2 Specific Objectives	3
2 State of the Art	5
2.1 sEMG Signals	5
2.2 Muscle Fatigue	7
2.3 Instrumentation of EMG	8
2.3.1 EMG Hardware and Software	8
2.3.2 Amplifiers	9
2.3.3 Digital instrumentation	10
2.3.4 Electrodes	10
2.4 Feature extraction	14
2.4.1 Time Domain	14
2.4.2 Frequency Domain	14
2.4.3 Time-frequency Domain	15

2.5	Fatigue Detection Methods	15
2.6	Fatigue Classification Methods	17
3	Methodology	21
3.1	Experimental procedure	22
3.2	Data Acquisition and Processing System	24
3.3	sEMG Signal Analysis System	28
3.4	Classification Models	33
4	Results	35
4.1	Feature Extraction Analysis	35
4.2	Classifier Models Performance	39
5	Discussion	41
6	Conclusions	45
6.1	Recommendations	46
6.2	Future works	46
	Bibliography	47
	Appendices	57
.1	Appendix 1.	59
.2	Appendix 2.	61
.3	Appendix 3.	63
.4	Appendix 4.	65
.5	Appendix 5.	66

List of Tables

2.1	An overview of some machine learning models used in the classification of fatigue and non-fatigue conditions.	19
3.1	Signal acquisition materials and their cost.	23
4.1	Summary of feature extraction analysis.	39
4.2	Classification performance of the extracted features for muscle fatigue detection.	40

List of Figures

2.1	Anatomical positions of selected electrode sites, frontal view. [1]	12
2.2	Anatomical positions of selected electrode sites, dorsal view. [1]	13
2.3	Changes in the quality of problem-solving depending on the amount of available data for machine learning algorithms of varying complexity [2]	18
3.1	Representation of the proposed method	21
3.2	sEMG signals acquisition in vastus lateralis (VL). (a) Schematic of the data acquisition process (b) Positioning of surface electrodes.	24
3.3	Data acquisition system	25
3.4	Command to save a signal	25
3.5	Biorthogonal 3.5 wavelet [3].	26
3.6	sEMG signal processing through the wavelet transform system.	27
3.7	Example of a sEMG signal processed using the wavelet transform system.	28
3.8	Feature extraction system. (a) Before Activity, (b) After Activity, (c) Scope to display.	30
3.9	Internal content of the "Feature Extraction" block	31
3.10	Functions for feature extraction (a) MAV, (b) RMS (c) MNF	32
3.11	Scope of MAV in each level processed with the DWT of participant 2 (first measurement). (a) Before activity, (b) After activity	33
3.12	Flow chart of the classification models	34
4.1	Mean Absolute Value of the participant 4 (first measurement). (a) Before activity, (b) After activity.	36
4.2	Root Mean Square of the participant 4 (first measurement). (a) Before activity, (b) After activity.	37
4.3	Mean Frequency of the participant 4 (first measurement). (a) Before activity, (b) After activity.	38

Abbreviations

A/D Analog-to-Digital.

AI Artificial Intelligence.

AR Autoregressive.

ARC Autoregressive model coefficient.

CMRR Common mode rejection ratio.

CWT Continuous Wavelet Transform.

DA Differential amplifier.

DWT Discrete Wavelet Transform.

EMG Electromiography.

FFT Fast Fourier Transform.

k-NN K-Nearest Neighbor.

MAV Mean Absolute Value.

ML Machine Learning.

MNF Mean Frequency.

MUs Motor units.

RF Random Forest.

RMS Root Mean Square.

sEMG Surface Electromiography.

STFT Short-time Fourier Transform.

SVM Support Vector Machine.

VL Vastus Lateralis.

VM Vastus Medialis.

WT Wavelet Transform.

WVD Wigner-Ville Distribution.

ZCR Zero-crossing rate.

Chapter 1

Introduction

1.1 Fatigue detection by using sEMG

Surface Electromyography (sEMG) is a common tool for detecting muscle fatigue and helps to program a suitable rehabilitation training plan. The sEMG signal is incredibly non-linear and non-stationary, and the acquisition strategy and external factors have a significant impact on it. In therapeutic sessions, it has always been difficult to successfully extract information about surface fatigue from sEMG signals [4]. There are numerous instances of sEMG signals being utilized to describe muscle fatigue in works of literature from the previous century. In 1912, Piper was one of the pioneering researchers to employ sEMG methods to monitor myoelectric symptoms of muscle exhaustion [5]. During isometric voluntary sustained contractions, he observed a progressive “slowing” of the EMG signal, which was actually a shift of the sEMG signals’ spectral components toward lower frequencies. Since then, EMG has been widely employed to assess muscle fatigue. sEMG techniques first focused on studying isometric or static contractions. It is simpler to record sEMG signals during isometric contractions in comparison with dynamic contractions. Since there is no movement during isometric contractions, there is less movement interference than during dynamic contractions. Although it is simpler to record sEMG signals during static contractions, there are still additional factors that could affect the recording of the signals and hence make it more difficult to interpret the results. These variables include the attenuation effect of the sEMG signal brought on by various subcutaneous tissue layer thicknesses, such as the fat tissue layer, or the various signal features that can be obtained depending on where the recording electrodes are placed over the muscle, such as close to tendons or innervation zones. Crosstalk, or the electrical activity of neighboring muscles, which can be captured using surface electrodes, is another important consideration [6]. In dynamic circumstances, the challenges of deciphering sEMG signals in static contractions are magnified. The joint angle doesn’t change while static contractions are occurring. On the other hand, when a dynamic contraction occurs, the joint angle shifts, moving the underlying muscle fibers away from the recording electrodes. The sEMG signal characteristics vary faster during a dynamic contraction compared to static contraction, as a result of additional effects during a dynamic contraction, such as quick changes in the recruitment and de-recruitment of motor units and variations in muscle force. Therefore,

the classic frequency techniques may not be suitable for extracting information and more sophisticated techniques may be required [6].

1.2 Problem statement

In recent years, electromyography (EMG) research has experienced remarkable growth. Advances in the biotechnology of sensor systems and data acquisition cards, as well as a solid understanding of the physiological behaviors of the human body, have contributed to the development of this type of research [7]. The detection of sEMG signals is frequently used in disciplines such as medicine, clinical diagnostics, and sports science, as they directly describe neuromuscular activity. The bioelectrical activity of the neuromuscular system during skeletal muscle contraction results in the production of the sEMG signal. Thus, this is an effective technique for determining muscle exhaustion since the variations of this signal coincide with the level of muscle activity and its functional state [8]. Knowing these signals can help in various fields such as rehabilitation medicine, sports medicine, physiotherapy [9], prosthetic devices, etc [10]. It is crucial to create supportive techniques to prevent loss of strength caused by muscle fatigue, as well as to identify it early and manage the situation more effectively [10]. This will help both clinical rehabilitation and injury prevention as muscle exhaustion increases the risk of sports injuries [11]. Commonly, sEMG signals are used to provide valid and reliable measurements during voluntary muscle contraction because it is a non-invasive technique. However, standardization of this detection method is required [7]. Some investigations use the Fast Fourier Transform (FFT) to analyze EMG signals, but this technique does not provide temporal data of the signal. On the other hand, high-frequency components have high temporal resolution due to the Wavelet Transform (WT), and low-frequency signals (such as transients) have high-frequency resolution. Despite the computational burden, the sensitivity to noise level and the dependence of its accuracy on the chosen wavelet are some of the disadvantages of the WT, according to some studies [12]. However, transformations are used to obtain additional information from a raw signal (i.e., in the time domain), and the WT of a signal is an effective method to represent the frequency and time information of a particular signal. In fact, the WT of a signal provides a two-dimensional representation of time and frequency. In addition, WT has been shown to outperform conventional methods for representing the time-frequency of a signal. These methods include the Wigner-Ville distribution and short-time Fourier transforms. The WT transforms signals with flexible resolution in the time and frequency domain [13]. Furthermore, since sEMG signals are non-stationary in nature, wavelet decomposition is the most suitable method to study these signals [8]. In general terms, WT was found to be a useful tool for processing time-varying and non-stationary signals, especially biomedical signals [13]. In this context, the present work proposes to address this problem by applying the wavelet transform to sEMG signals acquired before and after exercise in the gym, using the NI USB-6212 card and the MATLAB platform. This research aims to provide a significant contribution to the development of standardized methods for the detection of muscle fatigue, thus improving the understanding and practical application of sEMG signals in the sports environment.

1.3 Justification

The present work acquires outstanding relevance by contributing to the field of EMG signal analysis, specifically sEMG, which is applied to detect muscle fatigue in the vastus lateralis muscle. It is necessary to identify patterns and changes present in the signals in order to effectively evaluate the physiological and functional state of individuals subjected to physical effort, both within the medical and sports fields. For this purpose, an updated, safe, and scientifically proven technique will be assertive not only for injury prevention but also as a rehabilitation strategy. Therefore, the importance of this research lies in the understanding of sEMG signals and their application for the detection of fatigue, especially in the sports field, to optimize the performance of the individual and prevent injuries resulting from overexertion in exercise. In addition, the choice of approaching the analysis of sEMG signals in the vastus lateralis muscle using the wavelet transform responds to the need to find a method that can be standardized to evaluate these signals in a sports environment. This research justifies its relevance by providing a non-invasive, simple, and specific methodology that integrates the technology of the NI USB 6212 card and the MATLAB platform, allowing more accurate and detailed analysis of sEMG signals. The aim is, therefore, to fill this research gap and contribute to the consolidation of more effective practices in the evaluation of muscle fatigue, with direct implications for the improvement of clinical diagnosis and the optimization of sports performance. In addition, the vastus lateralis muscle was chosen because of its importance in the normal function of the knee joint. Furthermore, the prevention of lower body injuries is indispensable for most athletes in different sports disciplines, such as soccer, basketball, cycling, running, and gym training. Finally, most studies have been conducted on the upper body (biceps), so the focus of this study on the vastus lateralis may contribute to the literature of sEMG analysis for fatigue detection on the lower body and serve as a basis for future research.

1.4 Objectives

1.4.1 General Objective

The main objective of this research is to design a sEMG signal analysis system for fatigue detection in the vastus lateralis muscle by means of wavelet transform.

1.4.2 Specific Objectives

- To perform measurements of sEMG signals in the vastus lateralis muscle before and after the execution of gymnasium exercises in a group of people.
- Preprocess sEMG signals by applying the wavelet transform.
- Perform feature extraction of the sEMG signals before and after exercise and compare the results of both to identify patterns associated with muscle fatigue.
- Validate the proposed approach by comparing the results with other existing muscle fatigue detection methods.

Chapter 2

State of the Art

2.1 sEMG Signals

The electromyogram (EMG) has been extensively examined in medical and engineering fields, standing out as one of the most researched biosignals [14]. EMG represents muscle contraction in the human body. Fundamentally, this recording can be obtained through the use of sEMG or by using needle electrodes [12]. Skeletal muscles produce active forces for the static and dynamic motor processes of the human body by acting on the bone and joint system [15]. The electrical signals generated by skeletal muscles contain information about muscle activation and properties of the neuromuscular system since, before producing muscle force, muscle fibers produce electrical currents as a part of the signaling process of muscle contraction [16]. These signals are known as sEMG signals since they can be detected on the surface of the skin with the help of an EMG sensor and surface electrodes. These electrodes detect variations in voltage amplitude caused by motor activity, thus allowing the corresponding muscle activity to be captured [12]. The amplitude of a non-processed sEMG signal ranges between +/- 5000 uV [1]. It is influenced by several variables, such as the strength and timing of the muscle contraction, the distance between the electrode and the active muscle area, the characteristics of the overlying tissue, the design of the electrode and amplifier, and the effectiveness of the electrode contact with the skin [16].

In general, EMG signals are formed from the action potentials of sets of muscle fibers organized into motor units (MUs). It is important to know the number of active MUs because when there are 2 or 3 of them, they can be visually identified, but if there are 4 or more, they become indistinguishable. Decomposition of the EMG signal allows studying the temporal information of the MUs, which is useful in motor control research and the diagnosis of neuromuscular diseases [17]. On the other hand, sEMG signals do not only contain the signal originating from the muscles but also the endemic noise from various unavoidable components, which contaminates the sEMG signal and, if this noise is not eliminated or reduced, can lead to an error in the interpretation of the signal. Therefore, a bandpass filter is usually applied to preserve only the frequency spectrum of the desired signal as much as possible and obtain a more accurate sEMG signal [18]. It is essential

to determine the specific range that needs to be analyzed in order to obtain the relevant information and to reduce the noise. The best frequency range of the sEMG commonly fluctuates from 10 to 500 Hz [19] [20]. Thus, it is recommended to use an amplifier with a passband filter on that specific range. Moreover, the strongest sEMG signal is usually found between 10 and 250 Hz [1]. Therefore, the selection of the frequency range will depend on the target signal that needs to be measured, as well as the objectives of the study and its application. For instance, a study conducted by Correa et al. [21] focused on the development of a system of sEMG signal acquisition and processing for controlling robotics upper limbs and the EMG signal was filtered from 20 to 300 Hz by employing an integrator low-pass filter and a first-order high-pass differentiator (bypass filter). Thereby, commonly used EMG sensors come with a filter and can obtain a frequency spectrum ranging from 0 to 400 Hz, and for noise reduction in higher parts of the spectrum, a low pass filter with a cutoff frequency of 400-450 Hz is normally used [18]. Based on the literature, EMG signals need to be filtered between 10 and 20 Hz at the low-end and between 400 and 500 Hz at the high end. This allows to filter the noise while maintaining the intensity of the EMG signal [22].

The shape of the action potentials and the decay of the signal can be affected by the selected filtering method. A narrower bandwidth minimizes noise while improving the similarity between action potentials. To avoid fluctuating delays and keep the energy concentrated in short time lapses, zero-phase filters should be used. It is advisable to avoid using nonlinear filtering methods, as they can alter the EMG signals [22]. Low pass filtering helps to avoid signal aliasing and to remove high frequency components, while high pass filtering is necessary to remove low frequency motion artifacts. Historically, power line noise (50 or 60 Hz) was often removed by notch filtering, but this method can result in the loss of crucial EMG signal information and should generally be avoided [16]. Generally, low-frequency noise is produced by DC biases of an amplifier. In contrast to low-pass filter, high pass filters can usually be utilized to reduce this noise, which is produced by nerve conduction and is therefore more difficult to eliminate. In addition, both radio signals and computers produce high-frequency interference, which can be eliminated by using a low-pass filter. [10].

sEMG signals are collected from the skin surface and can be affected by various sources of electrical interference, such as electrical activity of the heart or motion artifacts. A cut-off frequency of approximately 30 Hz helps to reduce cardiac artifacts [23] [24]. For instance, in a feasibility study of neural networks for sEMG-based muscle force estimation, the raw sEMG data was filtered at a bandwidth of 20-500 Hz to remove low-frequency noise and motion artifacts [25]. On the other hand, an investigation runned out by Khan et al. [26] used Myo thalamic armband to acquire the respective signals from the muscles located under the elbow in order to present a sEMG dataset of routine activities, which can be useful for posterior researches on computing assistance for people with physical or mental disabilities. They employed a passband filter with a 5-100 Hz range frequency to reduce the noise and the influence of muscular movements. Some of the reasons for filtering electromyographic signals are to reduce interference from biological signals, to minimize electrical noise contamination, and to minimize baseline drift [24]. For example, Chang et al. [27] developed a wireless system of sEMG measurements with a sampling frequency of

2KHz. They applied Butterworth filters and high-pass filter (30 Hz cut-off frequency) to remove the displacement of the direct current, and the deviation of the baseline. Also, they implemented a low-pass filter (1kHz cut-off frequency) to reduce the high-frequency noise and avoid aliasing [27]. There are other cases in which the researchers have used a 20-450 Hz passband [28]. The most common biological signal that can interfere with the sEMG signal recording is the cardiac signal, especially when the measurements are conducted on the upper body muscles, which affects the amplitude of the signal and its strength [23]. Moreover, the deviation of the baseline can be caused by abrupt movements of the participant. Therefore, a passband filter with a cut-off frequency of 5 and 15 Hz needs to be used to reduce the influence of these movements and the influence of the electric line of 50 Hz and the T-wave [24]. Several factors need to be considered for the acquisition of sEMG signals such as previous skin preparation and the appropriate placement of electrodes to avoid altering the registered signal [24]. Finally, it is important to remark that the sEMG signal can also be affected if wrong and unnecessary filters are implemented, and the signal-noise relation should contain as much data as possible and the minimum noise pollution [29].

2.2 Muscle Fatigue

Muscle fatigue is the phenomenon produced by changes in the efficiency of the nervous system, as well as metabolic, structural, and energetic changes in the muscles caused by the lack of oxygen and nutrients [30]. It also involves the reduction of maximal muscle strength during contraction. Thus, it directly influences the capacity to move or lift weights. There are a wide variety of factors that can have an impact on fatigue levels, such as body energy supply, neurological issues, blood ion regulation, and muscle fiber composition, to name a few. In sports training and competition, a correlation has been found between the prevalence of musculoskeletal injuries and muscle fatigue. Muscle and bone injuries are more likely when fatigue is present because fatigue may change kinematics and muscle activation patterns [10].

During muscle contractions, fatigue is defined as a prolonged decrease in the ability to generate or maintain force at required levels. It can be caused by physical activity [31] following relatively heavy muscular activity [32], and produce a decrease in the maximal force of an isometric contraction during a maximal voluntary contraction [33]. The fatigue condition can also be described as a decrease in the ability of the neuromuscular system to generate force [10]. The two general types of fatigue are peripheral fatigue and central fatigue [34], both of which can contribute to neuromuscular fatigue [35]. The duration of a person's ability to perform a given amount of work can be used to gauge the onset of muscle exhaustion. Muscle capacity and power are reduced as a result of metabolite accumulation in the circulation during exercise, which causes exercise-induced muscle fatigue [11]. Besides, blood lactate concentration can also be measured during exercise, but this method does not allow real-time monitoring and only provides an estimate of the whole-body muscle fatigue [30]. In addition, when there is a lack of qualified neurologists, deep learning technologies can be utilized to identify and categorize neuromuscular fatigue [11]. sEMG analysis is the primary method to identify muscle fatigue because it allows

recording the signal of the target muscles and, therefore, obtaining the relevant data to do the analysis [10].

2.3 Instrumentation of EMG

The standardization of instrumentation and technical issues is vital in EMG, as this guarantees the high quality of the recordings. Its importance in the healthcare system have increased during the last years due to the rapid improvement of new technologies. Nowadays, most of the EMG equipment is digital and computerized, thus enabling greater instrumentation standardization. Technological advances in EMG equipment have helped EMG to remain as the most widely used method in routine clinical practice, even in developed countries. Diagnostic imaging methods, such as ultrasonography, have also come to be considered as a complement to electrophysiological studies and are utilized in EMG laboratories [36]. Additionally, Tankisi et al. [36] commented on the following details to be considered regarding the computer hardware to be used with the EMG instrumentation:

- Multiple displays allow to view the data from EMG signals together with other relevant information, such as data derived from additional tests or radiology.
- CPU speed and RAM capacity are determined by the EMG equipment manufacturer, who sets the minimum limits. The requirements vary according to the complexity of the software used.
- The size of the hard disk is defined by the EMG equipment manufacturer, who sets the minimum required limits. If you plan to store the data locally, the minimum hard disk size must be adequate for the approximate amount of data to be stored. Usually, more storage space might be needed at some point, so it is advisable to anticipate this situation.
- A loudspeaker is required to reproduce EMG signals when an EMG hardware unit is unavailable. Optimal sound quality is crucial to ensure accurate signal reproduction.

2.3.1 EMG Hardware and Software

The main function of the electrodiagnostic system is to record and analyze biological signals accurately. It is essential to maintain an optimal "signal-to-noise" ratio, which involves increasing the neurophysiological signal strength while simultaneously reducing background noise. To achieve this goal, analog hardware is used in conjunction with digital signal processing techniques. Signals and noise are captured by surface or needle electrodes and sent to the amplifier via electrode leads. These components have a similar functionality to that of an antenna, which can generate additional noise. A differential amplifier boosts the signal while attenuating unwanted noise with the help of analog filters. Subsequently,

the amplified signal is converted into a digital signal by an analog-to-digital (A/D) converter and the resulting voltage values are stored in the form of a matrix of numbers. This digitized signal facilitates subsequent analysis by performing computer methods [36].

In addition, some algorithms are capable of reducing noise, such as digital filters, averaging techniques, and smoothing, to name a few. There are also algorithms designed to perform specific measurements such as latency, amplitude, and area in nerve conduction studies. Some more advanced algorithms have the ability to identify motor unit potentials in needle EMG recordings. In addition, signal characteristics can be evaluated through their sonic representation generated by analog hardware or digital technology. An EMG machine also has stimulation devices designed to activate nerves and muscles. These devices can generate electrical, visual, or auditory stimuli. In addition, external devices can be connected to provide other types of stimulation, such as magnetic fields, contact heat, reflex hammers, etc. These external devices may be interconnected to provide synchronization signals through what are known as “triggers”. Sometimes, the equipment passes the digitized signals through a digital-to-analog converter to convert the digital signals, with a lower noise level, into analog signals. This can be useful in research in which is needed to resample the signals and develop algorithms for their own analysis [36].

The EMG machine displays the signals, measurements and settings of the amplifier and stimulator. The latter can be modified by means of a dedicated control panel or by software commands via the computer mouse or keyboard. On the other hand, the software takes care of signal processing and report generation. Furthermore, it can create databases and allow remote reviews for second opinions or interpretation assistance. Additionally, EMG analysis software can offer available tests and functions that optimize workflow and are compatible with local practices and reference limits. It may also include a help function covering strategies and signal quality control. [36].

2.3.2 Amplifiers

The amplifier plays a fundamental role in the quality of electrodiagnostic systems. Webster [37] stated that in order to achieve selective amplification of a neurophysiological potential while attenuating background noise, a differential amplifier (DA) must be used. This type of amplifier requires three-electrode inputs or connections, commonly labeled ‘E1’, ‘E2’, and ‘E0’ [38] [39]. Generally, the standard colors of these inputs are black (E1), red (E2), and green (E0) [36], also known as ‘active’, ‘reference’ and ‘ground’ respectively [36] [39]. It is named DA because the amplifier does not directly amplify the voltage at inputs E1 or E2, but amplifies their difference instead [36]. A DA must have high differential gain and low common mode gain for accurate measurement of biopotential signals [37]. This can be summarized in a characteristic called common mode rejection ratio (CMRR). Modern electrodiagnostic systems have amplifiers with a CMRR greater than 100 dB, although it is important to note that the CMRR decreases at higher frequencies usually specified at 50 or 60 Hz (the power line frequency) [36].

Another characteristic of the amplifier is the input voltage range, which defines the

range of signal amplitudes that the amplifier can handle without distortion. It is essential to set the amplifier range above the expected amplitudes of the signals recorded during the test to avoid saturation and ensure accurate measurements. A high amplifier range and a narrow bandwidth contribute to reduce noise. Furthermore, the amplifier is also characterized by its input impedance, which must be significantly higher than the impedance of voltage generators, such as muscles, nerves or body fluids, to minimize noise sensitivity and avoid underestimating the signal amplitude. Fortunately, modern systems generally report impedances in excess of 100 to 1000 mega Ω , but like CMRR, impedance decreases at higher frequencies. Additionally, it is critical to reduce ambient noise and ensure that there are no significant differences in noise between the E1 and E2 electrodes to obtain high-quality recordings [36].

2.3.3 Digital instrumentation

EMG systems use digital computers to perform data sampling, storage and signal processing. Once the analog signal has been amplified, the A/D converter discretizes the signal in both time and amplitude, assigning a digital value to the amplitude at specific time points. This assignment of the amplitude to a digital value is carried out by using a finite number of digital amplitude values. During this conversion process, two important conditions need to be satisfied. First, the sampling frequency must be high enough to accurately represent the original analog signal. And secondly, the amplitude digitization must be fine enough to represent the amplitude of the original signal accurately in the digital domain. Moreover, by using appropriate algorithms, it is feasible to reconstruct the waveform in detail if the sampling rate is greater than twice the highest frequency present in the waveform, as stated by Nyquist's theorem. Furthermore, the sampling frequency that is usually used in practice ranges from 2 to 5 times the highest frequency of the signal of interest. In addition, to ensure that the maximum frequency of the signal is known, an analog "anti-aliasing" filter is applied before digitizing the signal. The number of bits required for the A/D converter is determined by the target amplitude resolution and the maximum amplitude of the signal [36]. Currently, A/D converters are available up to 24 bits or more, enough for most biomedical applications [40].

2.3.4 Electrodes

Standard electrophysiological recordings involve the use of at least two electrodes, because they are differential recordings. In unipolar or referential recordings, the active electrode (E1) is placed close to the active fibers or any fibers of interest, and the reference electrode (E2) is located at some distance in a region with minimal activity. However, although these types of recordings imply that the recording area is electrically silent, sometimes, especially when recording certain surface motor responses, the reference electrode may detect volume-conducted electrical activity. In bipolar recordings, both electrodes are placed close to the active fibers. There are also recordings which use a common reference, in which three electrodes (E1, E2, E0) are used. In the latter case, the third electrode is connected to ground to establish a constant voltage reference point. In addition, the most

common electrode materials used are platinum, stainless steel and silver-silver chloride. Most surface electrodes need a conductive medium to guarantee adequate electrical contact with the skin; it can be electrode gelatine/paste, saline solution or an adhesive gel. In addition, identical electrode materials have to be used to minimize electrode contact impedance mismatch, in order to reduce the signal-to-noise ratio [36].

In some cases of EMG, a concentric needle is commonly used, consisting of an outer cannula that serves as the reference electrode and an inner core that functions as the active electrode. The concentric needle is composed of two electrodes: a wire electrode, usually made of platinum, that is insulated, housed within a steel cannula that acts as a second electrode. Differential recording is achieved by measuring the potential difference between the wire electrode (active electrode, E1) and the entire cannula shaft (reference electrode, E2). Alternatively, monopolar needles can be used, where the conical tip of the needle acts as a single electrode. Monopolar needles for EMG recordings are usually made of a Teflon-coated stainless steel core, except for a 1-5 *mm* exposed conical tip that acts as the active electrode. The recording area ranges from 0.03-0.34 *mm*². Potential difference is measured from the exposed tip of the needle to a second reference electrode. This reference electrode can be a subcutaneously placed needle or a surface electrode at some distance from the active electrode. The reference electrode should be positioned over an electrically silent area, such as a tendon or bone. Impedance mismatch between the active monopolar needle and a surface electrode can cause a reduction in the common mode signal and increase artifacts, including power line interference. Monopolar needles record higher amplitudes and durations than concentric needles, but the number of phases is comparable. Surface electrodes have various uses for both stimulation and recording in nerve conduction studies, and allow the capture of sEMG data. They are usually silver-silver chloride electrodes, with a conductive adhesive gel on the electrode surface. They can be reused on a few occasions in the same patient until the effectiveness of the adhesive decreases and needs to be replaced. To record finger sensory potentials, reusable electrodes made of a Velcro band impregnated with saline solution can be also used [36].

Most of the important muscles of the limbs and trunk can be measured with surface electrodes. Still, deeper, smaller, or overlapping muscles need the application of fine wire to be selectively detected. Considering the muscles normally investigated in kinesiological studies, Konrad et al. [1] show the muscle maps with reference to the recommended position for fine wire and surface electrodes. Figure 2.1 shows the anatomical position of selected electrode sites in the frontal view, while Figure 2.2 shows the anatomical position of selected electrode sites in the dorsal view. In both, the left side indicates the position for fine wire electrodes and the right side displays the adequate location for surface electrodes. The two yellow dots placed on the superficial muscles represent the orientation of the electrode pair relative to the direction of the muscle fiber. Additionally, one neutral reference electrode must be placed per subject. For this purpose, a nearby area should be selected that is not electrically affected, e.g., joints, bony area, spinous process, tibia bone, iliac crista, frontal head, etc [1].

Fine Wire Sites:

Surface Sites:

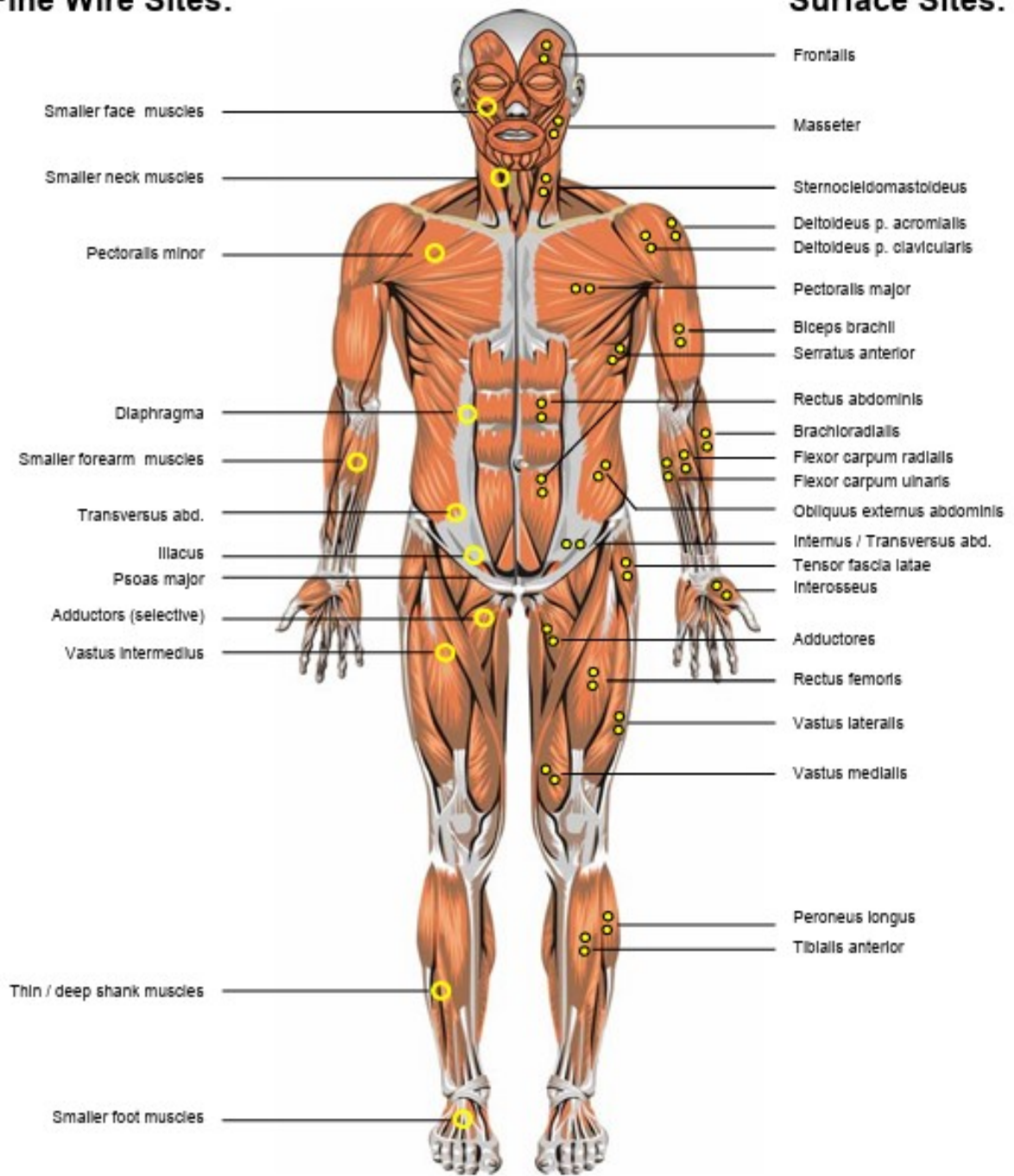


Figure 2.1: Anatomical positions of selected electrode sites, frontal view. [1]

Fine Wire Sites:

Surface Sites:

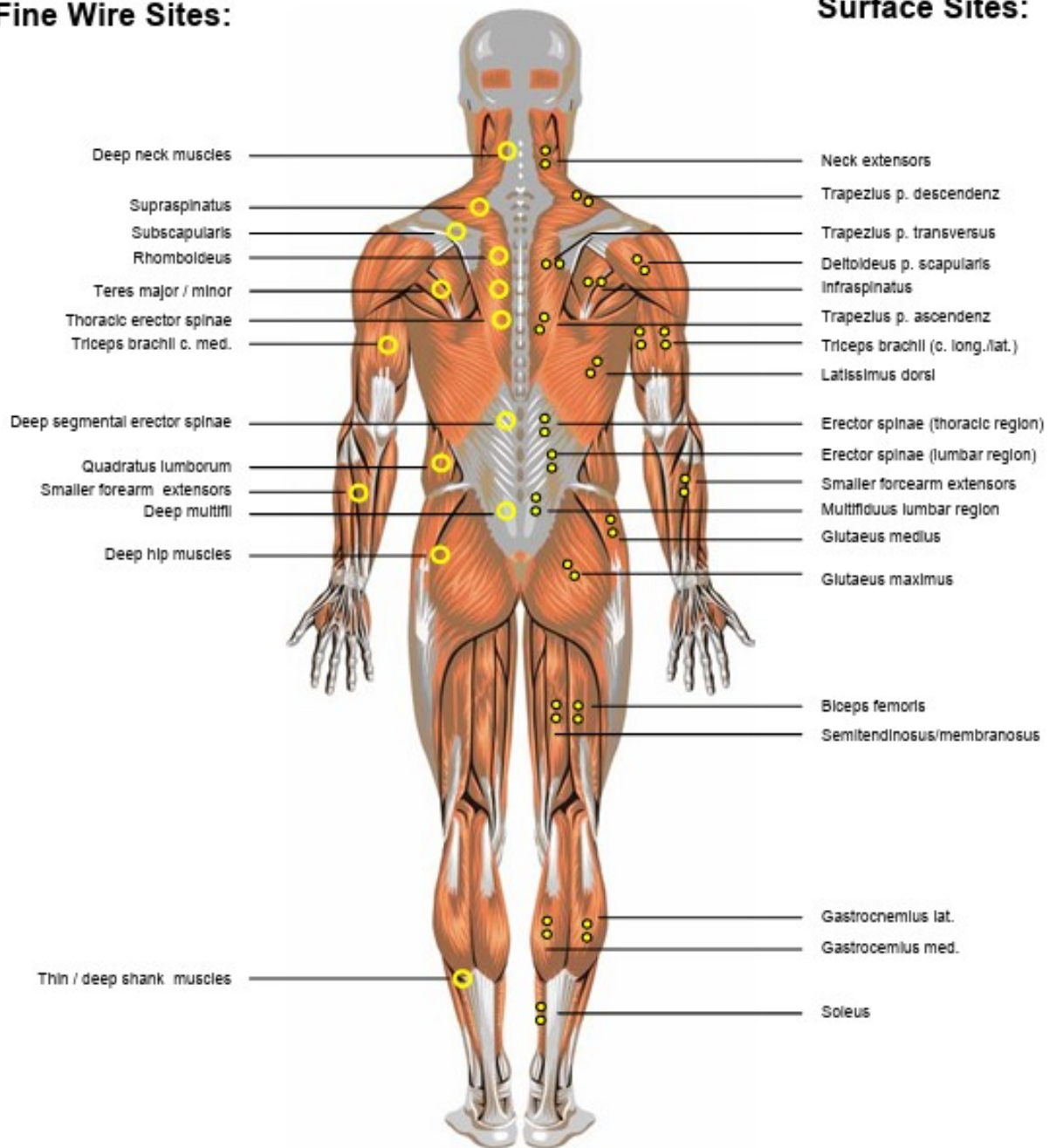


Figure 2.2: Anatomical positions of selected electrode sites, dorsal view. [1]

2.4 Feature extraction

Feature extraction is a technique for extracting meaningful information from EMG signals during fatigue. Whenever there is a mutual decrease of the investigated parameter in the frequency domain and in the time-frequency domain, as well as an increase of the evaluated parameter in the time domain, the EMG signal usually detects muscle fatigue [10]. The characteristics of EMG feature space, such as maximum class separation, resilience, and computational complexity, should be taken into account to achieve the best classification. Time-domain, frequency-domain and time-frequency domain features are the three different forms of EMG features [41]. In particular, it is considered that the two reliable indicators of muscle fatigue are the time-domain and frequency-domain characteristics. Additionally, it is important to adopt a suitable signal processing method to deal with non-stationary signals for fatigue detection, this will allow to extend the studies within the field of sports, rehabilitation, and assistive devices [42].

2.4.1 Time Domain

The EMG signal is filtered in the time domain to reduce noise and crosstalk. While an increase in EMG amplitude is associated with muscle fatigue, Mean Absolute Value (MAV) and Root Mean Square (RMS) characteristics can also be used. In addition, it is advisable to combine amplitude-based detection with spectrum analysis or other techniques since amplitude detection alone is not accurate. The relationship between signal amplitude and muscle force is influenced by various depletion regimes. To improve detection, the use of multiple time windows (MTW) with various functions is suggested [10]. Different temporal domain methods have been investigated for the study of sEMG signals, with a particular focus on sEMG amplitude estimations, zero-crossing rate (ZCR), and spike analysis. Due to muscle tension and exhaustion, amplitude modulation is the most significant shift in the temporal domain of the sEMG signal. The MAV and RMS are two often used metrics. Five successive processing steps—noise rejection/filtering, whitening, amplitude demodulation, smoothing, and relinearization—have been utilized in a cascade to estimate the sEMG amplitude. Half of the signal's zero crossings per second is considered the ZCR. Due to ZCR's, sensitivity to amplitude distribution and signal-to-noise ratio are no longer used. In order to provide information similar to that of spectral analysis without requiring stationarity, peak analysis emerges as a rarely utilized technique in sEMG signal analysis which involves the identification of peaks and variations within peaks. However, the utilization of sEMG peak parameters has been constrained by contradictory results about their dependability [30].

2.4.2 Frequency Domain

Analysis of the EMG signal reveals a shift in the frequency spectrum toward lower frequencies as a result of muscle fatigue. The initial non-fatigued state has been used to relate

these changes using metrics such as mean and median power frequencies [10]. One of the most commonly used frequency characteristics is the mean frequency (MNF) [30]. The phenomenon of MNF and median frequency (MDF) shift of the sEMG toward lower frequencies during the isometric condition has been used as an indicator to record the altered fatigability of the vastus lateralis (VL) and vastus medialis (VM) muscles [43]. In addition, it has been observed that decreased muscle work during recurrent exercise is associated with reduced peak frequencies of certain muscles. However, combining frequency analysis with time domain characteristics is advisable to obtain more complete data on muscle function for more accurate identification of fatigue [10]. In order to analyze sEMG signals in the frequency domain, it is necessary to look at how the signal's spectrum evolves during prolonged contractions. The power spectral density of the sEMG signal can be calculated using Fourier-based spectral estimators, such as the periodogram. Autoregressive moving average (ARMA) models are used by parametric-based spectral estimators to explain the stochastic process underlying the sEMG signal. In real life, these techniques are employed to assess muscular fatigue. In EMG investigations, the autoregressive (AR) model is frequently used, and the right model order can be established utilizing a variety of factors. In general, these frequency domain techniques offer insightful information about muscle fatigue during prolonged voluntary or electrically evoked contractions. Depending on the particular application and signal parameters, other model orders might be appropriate. For example, among elite rowers, lower back pain has been detected via frequency analysis of myoelectric signals, showing the real applicability of performing sEMG on the biomedical field [30].

2.4.3 Time-frequency Domain

The combined analysis of EMG spectrum and amplitude occur because of the relationship between muscle fatigue and certain properties of the EMG signal. Various time-frequency approaches, such as Short-Time Fourier Transform (STFT) and CWT, are used to investigate muscle fatigue. These methods can simulate spectrum compression during exhaustion. The use of various traditional and contemporary techniques, including time-frequency scale approaches, RMS, wavelet analysis, and MNF, allows for a comprehensive assessment of muscle fatigue [10]. Analyzing sEMG data during static and dynamic muscle contractions involves using time-frequency and time-scale approaches. Fourier-based spectrum estimators, like spectrograms, are used for static contractions [30]. Methods like the Choi-Williams transform, which circumvents some spectrogram restrictions and offers improved time and frequency resolution for non-stationary signals, are being investigated for dynamic contractions [44]. These methods have been used to examine how muscles become fatigued throughout different actions and activities. They make it possible to assess the electrical signs of exhaustion and offer insightful data on how muscles behave under various conditions [30].

2.5 Fatigue Detection Methods

Different methods of sEMG signal analysis have been developed in order to assess fatigue in diverse muscles under a wide variety of contraction conditions [42]. Power spectrum

parameters can be obtained by using techniques such as FFT and other traditional signal processing methods, but these methods may not be appropriate for sEMG analysis of the force-varying muscle contractions due to the dynamic nature of these contractions [42]. Numerous methods have been developed to overcome the difficulties associated with the analysis of nonstationary muscle contraction and fatigue assessment, focusing on time-frequency or time scale. For example, one such approach is Cohen's Class, a widely used representation in time-frequency analysis, which was first proposed by Cohen [45] through the use of bilinear transformations. Despite its usefulness, Cohen's Class can be susceptible to cross-term contamination, which can affect the accuracy of the results [42].

The variability of sEMG signals poses challenges in their analysis. Applying the Fourier Transform to extract frequency characteristics results in a loss of temporal information. In addition, sEMG signals do not meet the stationarity requirement of the Fourier Transform, which makes their direct analysis difficult. To solve this problem, it is used the STFT, a variant of the Fourier transform that is computed using a sliding time window. This approach allows to analysis of temporal variations in the sEMG signal spectrum, thus meeting both frequency and time requirements in its analysis [30]. In an investigation examining the comparison between STFT and continuous wavelet transforms (CWT) in the analysis of sEMG signals from back and hip muscles during fatiguing isometric contractions, it was found that both methods provided similar information about the spectral characteristics of EMG signals and, consequently, STFT can still be used [46].

Wigner-Ville Distribution (WVD) is an effective technique for analyzing non-stationary signals, offering higher time and frequency resolution than the spectrogram, overcoming some of its limitations [42]. In another investigation where they used the WVD method to examine the electrical activities of the uterine muscle and track its instantaneous frequency, it was found that this method of time-frequency analysis has limitations due to considerable cross-terms or interferences between elements present in different time and frequency areas [47]. Another study used the Choi-Williams transform for the processing of surface myoelectrical signals recorded during dynamic contraction to evaluate the electrical manifestations of muscle fatigue, extracted the instantaneous spectral parameters suitable for tracking changes caused by muscle fatigue, and found that this method provided useful information on the evolution of the frequency content of these signals[44].

The wavelet transform (WT) is an alternative method for the analysis of time-varying signals, such as the STFT, by replacing the frequency shift operation with a time-scaling operation. The wavelet transform is often used for signal decomposition and reconstruction [48]. It can also be used in non-stationary conditions since it varies the time-frequency relationship and can provide good frequency localization at low frequencies and good time localization at high frequencies. In addition, WT guarantees good time resolution at high frequencies and good frequency resolution at low frequencies, unlike STFT which has fixed time and frequency resolution and cannot inherently provide good time resolution along with good frequency resolution [49]. Furthermore, Karlsson et al. ([50]) described that the WT functions as a mathematical microscope that allows observing different aspects of the signal by adjusting the focus. They compared the STFT, WVD, the Choi-Williams distribution, and CWT to determine their precision and accuracy and found that the estimates

provided by the CWT were more precise and accurate than those of the other methods on the simulated data sets. Furthermore, in their previous fatigue study involving maximal knee repetitions in isokinetic extensions, CWT showed that the frequency components were shifted toward lower frequencies. This methodology also makes it possible to analyze changes in frequency components throughout the range of motion during dynamic contractions. [51]. The CWT has a variable time-frequency resolution, which guarantees good time resolution at high frequencies and good frequency resolution at low frequencies [30]. Furthermore, in a study based on the use of CWT to examine motions at various angular velocities with surface myoelectric signals, it was concluded that this method is reliable in the analysis of non-stationary biological signals and without the need to apply smoothing functions [51].

Another statistical method known as the AR model is used as a signal processing tool to estimate natural behaviors using a random process [42]. An investigation to analyze the performance of the first autoregressive model coefficient (ARC) in assessing trunk muscle fatigue found that ARC could become a potential parameter to describe trunk fatigue during static and dynamic contractions [52]. On the other hand, feature extraction from sEMG signals with the use of the wavelet package and neural networks has also been shown to be useful in the identification and classification of muscle fatigue by using wavelet coefficients as features for fatigue identification, and self-organizing map neural network as a visualization and detection tool [53]. WT decomposes a signal into a series of wavelets. In addition, it has been considered that signals processed by the WT can be stored more efficiently compared to those signals that have been processed using the Fourier transform [53]. Another important fact to consider is that the biorthogonal mother wavelet is suitable for performing electromyography (EMG) as a basis function [54]. Moreover, the preprocessing of sEMG signals by Discrete Wavelet Transform (DWT) has been shown to be consistent and stable for identifying low-level fatigue [55]. The DWT method has been demonstrated to be effective in the analysis of non-stationary signals [41]. It is known that the DWT is an efficient technique for representing and analyzing biomedical signals, and it is commonly used to attenuate the noise in these signals [56].

2.6 Fatigue Classification Methods

Artificial Intelligence (AI) is the capability of a digital computer or computer-controlled robot to carry out tasks typically attributed to intelligent beings [57]. AI involves areas such as Machine Learning (ML), natural language processing, robotics, vision, etc [2]. ML represents a set of techniques within the field of AI that enable computer systems to acquire knowledge from past experience, i.e., by observing data, and improve their performance in executing a specific task. Besides, ML approaches include support vector methods, decision trees, Bayesian learning, k-means clustering, association rule learning, regression, and neural networks, etc [58]. In addition, ML methods can solve problems of regression, classification, clustering, and dimensionality reduction of data [2]. The most appropriate classification algorithm to use will depend on the amount of data available. In Figure 2.3, a scheme made by Mukhamediev et al. [2] is shown, which indicates that traditional algo-

gorithms are more efficient when dealing with small databases, and neural networks for large databases. Traditional classification methods include k-Nearest-Neighbor (k-NN), Logistic Regression (LR), and Decision Tree (DT), to name a few. Moreover, Table 2.1 presents some works in which they have tested the use of different machine learning models for the classification of fatigue and non-fatigue conditions in sEMG signals.

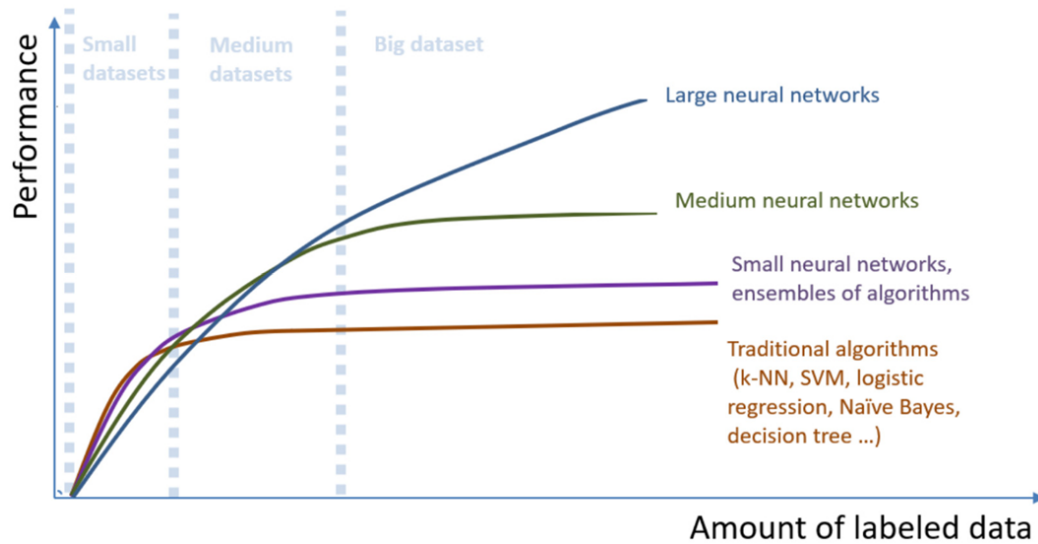


Figure 2.3: Changes in the quality of problem-solving depending on the amount of available data for machine learning algorithms of varying complexity [2]

Table 2.1: An overview of some machine learning models used in the classification of fatigue and non-fatigue conditions.

Ref.	Classification Method	Finding
[59]	CNN-SVM, Support Vector Machine (SVM), CNN, and Particle Swarm Optimization Support Vector Machine	The CNN-SVM algorithm achieved accurate muscle fatigue classification and 80.33% -86.69% classification accuracy.
[11]	Long short-term memory (LSTM) network, CNN, and SVM	The best performance of the LSTM network was achieved with 70% training, 10% validation, and 20% testing rates.
[60]	DEWOA-SVM, WOA-SVM, GWO-SVM, DEGWO-SVM, PSO-SVM, and FA-SVM	Results demonstrate the effectiveness and feasibility of the DEWOA-SVM method in dynamic muscle fatigue prediction with an average accuracy of 85.50% in ankle dorsiflexion and 84.75% in ankle plantarflexion.
[61]	Naive Bayes (NB), SVM, k-NN, and Linear discriminant	k-NN algorithm is found to be the most accurate in classifying the features with a maximum accuracy of 93%.
[62]	3 types of LR classifiers: Linear logistic, Polykernel logistic regression and Multinomial regression with ridge estimator	All classifiers are found to be useful in discriminating the output labels. However, based on the values of the classifier performance indices, the Kernel Logistic Regression algorithm is comparatively superior.
[63]	k-NN, NB, and LR	The LR and kNN classifier performance gave an accuracy of 84% and 82%, respectively.
[64]	NB, SVM of polynomial and radial basis kernel, Random Forest (RF) and rotation forests	The combination of EMBD- polynomial kernel based SVM is found to be most accurate (91% accuracy) in classifying the conditions with the features selected using genetic algorithm (GA).
[65]	k-NN, and LR	The classification accuracy with conventional features in dynamic contraction is 75% (improved to 80% with k-NN GA combination).
[66]	k-NN, NB, Decision tree, and Multilayer perceptron (MLP)	Maximum accuracy of 86% is achieved with MLP based detection model.

Chapter 3

Methodology

In this chapter, the methodology used for the proposed method for detecting fatigue in the VL based on the analysis of sEMG signals is presented, which is represented in Figure 3.1. First, Section 3.1 details participants information, materials used as well as their cost, and instructions prior to signal acquisition. Section 3.2 explain the mechanism of the signal acquisition system and the data processing system. In Section 3.3, the feature extraction system used for signal analysis is shown. Finally, Seccion 3.4 mentions the traditional ML models used for classifying fatigue and non-fatigue conditions.



Figure 3.1: Representation of the proposed method

3.1 Experimental procedure

To select the participants, factors such as age, weight, and health status were taken into account. First, Ayramo [67] suggested on his research that kids (age: 11-14 years old; weight: 47.9 ± 7.1 kg) need less time to recover from exercises, and they are less prone to present fatigue in comparison to youngsters (age: 14-16 years old; weight: 63.9 ± 4.2 kg) and adults (age: 18-24 years old; weight: 73.2 ± 7 kg). In addition, Tibana et al. [68] confirmed that youngsters (age:14-16 years old; weight: 61.1 ± 6.8 kg) depict more resistance to fatigue than the adults (age: 19-25 years old; weight: 71.2 ± 7.5 kg). Furthermore, several studies agree in the conduction of a research about fatigue in healthy patients without any cardiovascular and neuromuscular diseases or any other pathology [59] [69] [8] [70] [64]. Considering these factors, participants were selected who met the average characteristics of the adults in the aforementioned studies [67] [68]. During the performance of the present experiment, ten healthy people, without cardiovascular or neuromuscular diseases and any pathology, participated (7 males and 3 females, age: 18-23 years old, mean age: 20.8, mean height: 1.65 m; mean weight: 65.2 kg). All participants participated voluntarily, knew the purpose of the study and all the research details, and signed an informed consent form shown in Appendix.1. The study was conducted in Urucuquí-Ecuador. Two measurements were taken per participant, with the second measurement being carried out three days after the first measurement. In addition, the materials and cost of the prototype used in this work in order to acquire the signals are detailed in Table 3.1. Three Ag-AgCl surface electrodes were used per person. The data acquisition board has a 16-bit analog input resolution, maximum sampling rate of 400kS/s, USB 2.0 bus connector, and multifunction (I/O). All the equipment used was properly calibrated. Signal acquisition was performed on an AMD Ryzen 5 5600G computer and a 12 GB memory card, and experimental data analysis was performed on an Intel Core i5-1135G7 and an 8 GB memory card. Data were recorded using the laptop computer through the USB A/D converter interface, NIDAQ USB-6212 (<https://www.ni.com/es-cr/shop/model/usb-6212.html>). The systems used for signal acquisition, processing, and analysis were designed and implemented in MATLAB and Simulink.

For the present study, it was decided to work with a quadriceps femoris muscle, which is composed of the VL, VM, and rectus femoris, because this muscle group plays an important role in the normal function of the knee joint [71] and the patellofemoral joint [72]. In addition, knee injuries are common in various competitive sports and can limit an athlete's ability to continue practicing their discipline or, in the worst-case scenario, abruptly end their sports career [73]. The mechanomyographic signals of the VL and VM tend to compress toward lower frequencies with increasing isometric force, suggesting that these muscles may be more sensitive to fatigue compared to the rectus femoris [74]. Moreover, based on the EMG measurements, it can be noticed that the changes in the neuromuscular function of the VL and VM are related to the patellofemoral pain [75]. The muscle chosen to carry out this study was the VL, because it has a larger cross-sectional area compared to the VM [76], which facilitates accessibility for electrode placement and accurate measurements. Before the test, the participants were asked to shave the skin hair in the leg area since this is necessary for the electrodes to adhere better and reduce impedance [11]. Subsequently, the area was first cleaned with medical alcohol, and then the sEMG

Table 3.1: Signal acquisition materials and their cost.

Qty	Name	Unit Price (\$)	Total Price (\$)
1	NI USB-6212 Data Acquisition Card	1902.6	1902.6
1	EMG sensor	52.65	52.65
2	18650 Battery Holder	7.25	14.50
1	Cable for EMG sensor	14.99	14.99
1	ECG electrodes package (50 pcs.)	20.00	20.00
4	18650 batteries	7.85	31.40
1	18650 battery charger (2 channels)	30.00	30.00
1	Electronic parts	45.00	45.00
1	Laptop	800.00	800.00
	Total		2911.14

electrodes were placed in the VL muscle. For the proper positioning of the electrodes, the SENIAM guidelines [77] were taken into account, as well as information from the literature concerning the placement of the electrodes in the VL [78] [79]. The schematic of the sEMG signal acquisition process and the location of the electrodes is shown in Figure 3.2.

It is known that in EMG, almost all the signal power is between 10 and 250 Hz and scientific recommendations (SENIAM, ISEK) demand an amplification band setting of 10 to 500 Hz [80] [81]. A sampling frequency of 1500 Hz would be recommended to avoid signal loss [1], but it should be 2 KHz if the mean frequency is going to be used to evaluate muscle fatigue [27]. Based on this, the sampling frequency in this study was 2000 Hz. Pre-exercise and post-exercise measurements were taken while the subject was generating maximal voluntary contraction during isometric standing contraction for 20 seconds. The participants performed the exercises in the Yachay Tech University gymnasium under the supervision of a coach. This study focuses on gym activities since it is common for an imbalance between metabolic energy production and consumption to occur due to physical intensity. This imbalance leads to the accumulation of metabolic waste at the cellular level, causing the body to go out of its normal balance (homeostasis). Previous research on overtraining in athletes suggests that fatigue often develops before muscle injury occurs because muscles in this state are more susceptible to damage [82]. In addition, it is important to consider that for strength exercises to be really effective, the muscles need to be activated at least 40-60 % of their maximum capacity. This is essential to achieve a positive increase in strength due to super compensation, which is basically muscle growth in healthy people [1]. So, to activate the VL muscle, the exercises performed focused on strengthening the quadriceps since the VL is one of the main muscles of this group. The exercises performed by the participants were squats, leg presses (lying), leg extensions, lunges, and step-ups.

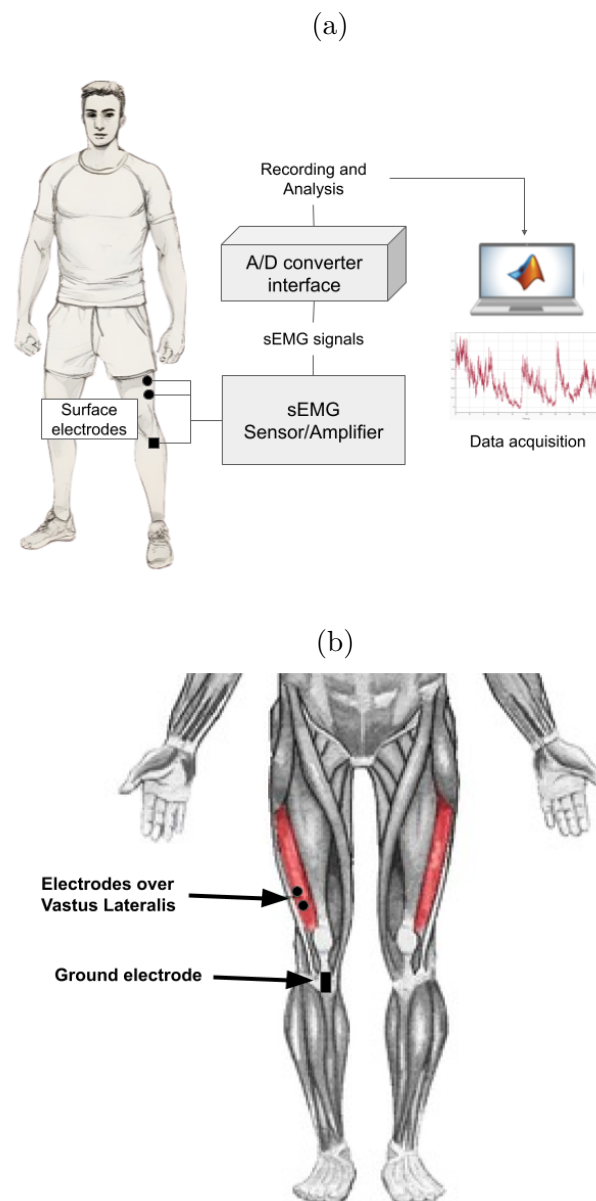


Figure 3.2: sEMG signals acquisition in vastus lateralis (VL). (a) Schematic of the data acquisition process (b) Positioning of surface electrodes.

3.2 Data Acquisition and Processing System

Data Acquisition toolbox is required, and it is necessary to register our hardware. Therefore, we log in as administrator in Matlab and run DAQSUPPORT to register all the adapters that have hardware installed. We then log in as a standard Windows user and can make use of the installed hardware with the Data Acquisition toolbox. Finally, Simulink was used to create the signal acquisition system, which is shown in Figure 3.3. The “Analog Input” block allows the analog data connected to the DAQ input ports to be read, the “Scope” element is used to display the acquired signal, and the “To Workspace” element

creates a variable that stores the acquired data so that it can be saved [83]. Figure 3.4 it is detailed how to save the signal, in this case, the first signal taken before the exercise was named “p1ae1” and was assigned the values previously recorded in the “To Workspace” element. Press Enter, and the signal will be saved in the computer with file type “.mat”. We repeat the process for each signal but with the corresponding name.

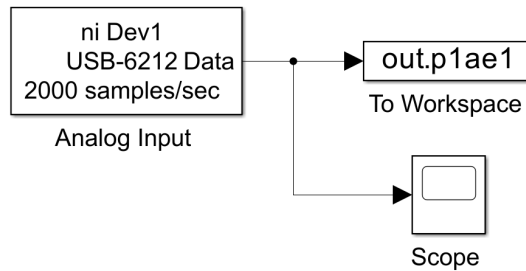


Figure 3.3: Data acquisition system

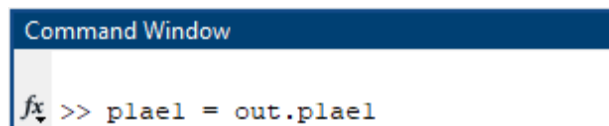


Figure 3.4: Command to save a signal

The unfiltered and unprocessed signal is called the raw sEMG signal and contains interfering components that make it difficult to analyze [1]. Although bandpass and lattice filters are commonly used to remove noise from raw sEMG signals, this can distort the signal and remove useful information from the sEMG signal. Therefore, the recommended method for removing artifacts from biomedical signals is the WT, which consists of decomposing and reconstructing the signal by removing undesired artifacts [56]. WT has proven to be a useful tool for sEMG signal processing and has been shown to be better than other traditional methods because of its flexible resolution in the time domain and frequency domain [13]. There are two types of WT: CWT and DWT [84]. DWT has less computational complexity and is faster compared to CWT [13]. In addition, one of the main advantages of DWT is its ability to generate a useful subset of frequency components or scales from the signal of interest [84]. Consequently, the DWT was used in the present work for processing the raw signals, whose general equation, according to Chowdhury et al. [41], is given by Equation 3.1. The wavelet mother used to attenuate the noise of the sEMG signal was the biorthogonal 3.5, whose graphical representation is displayed in Figure 3.5 and shows its similarity to a biosignal. Although it has not been commonly used for sEMG signal processing and analysis for fatigue detection to date, its use is proposed because of its good performance, feature extraction capability, and contribution to accurate classification [85]. In addition, the biorthogonal 3.5 has been noted for its efficiency in removing electrocardiographic interference in signals with a signal-noise relation of 30 to 75 dB, making it a good choice for implementation in filtering systems [86]. Moreover, a biorthogonal mother wavelet is considered useful for representing and decomposing EMG

signals [54].

$$x(t) = \sum_{k=-\infty}^{\infty} \sum_{l=-\infty}^{\infty} d(k, l) 2^{\frac{k}{2}} \psi(2^{-k}t - l) \quad (3.1)$$

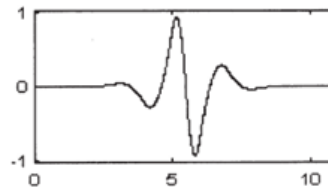


Figure 3.5: Biorthogonal 3.5 wavelet [3].

The Wavelet Toolbox was required for the system development in Matlab. The system was developed in Simulink and is shown in Figure 3.6. First, it is necessary to enter the sEMG signal in the “Signal input” component from workspace. The “Buffer” component converts the signal data sequence into a frame sequence at a lower frame rate, i.e. it provides a temporary storage of the signal, adjusts the sampling rate and facilitates signal preprocessing. Inputs are always interpreted as frames. The frame size must be a multiple of 2^n ; in this case, the output buffer size (per channel) is 256. The “DWT” component represents the Dyadic Analysis Filter Bank block and calculates the discrete wavelet transform; that is, it decomposes a signal into subbands with smaller bandwidths and slower sampling rates. The parameters used are biorthogonal filter, filter order [3/5], 4-level, and asymmetric tree structure. The Output parameter is set to multiple ports, so the block outputs each subband from a different port as a vector or matrix, and the top port outputs the subband with the highest frequency band. The “Delay” component was also implemented, which delays the input signal by a specified number of samples. The delay values were calculated following the source [87]. The “IDWT” component represents the Dyadic Synthesis Filter Bank block. It calculates the inverse discrete wavelet transform, which means it reconstructs the signal from subbands with smaller bandwidths and slower sampling frequencies. The IDWT parameters are the same as those used in the DWT. The “Unbuffer” component converts a frame into scalar output samples at a higher rate. The “Scope” was used to visualize both the initial signal and the processed signal with the mathematical model of the wavelet transform.

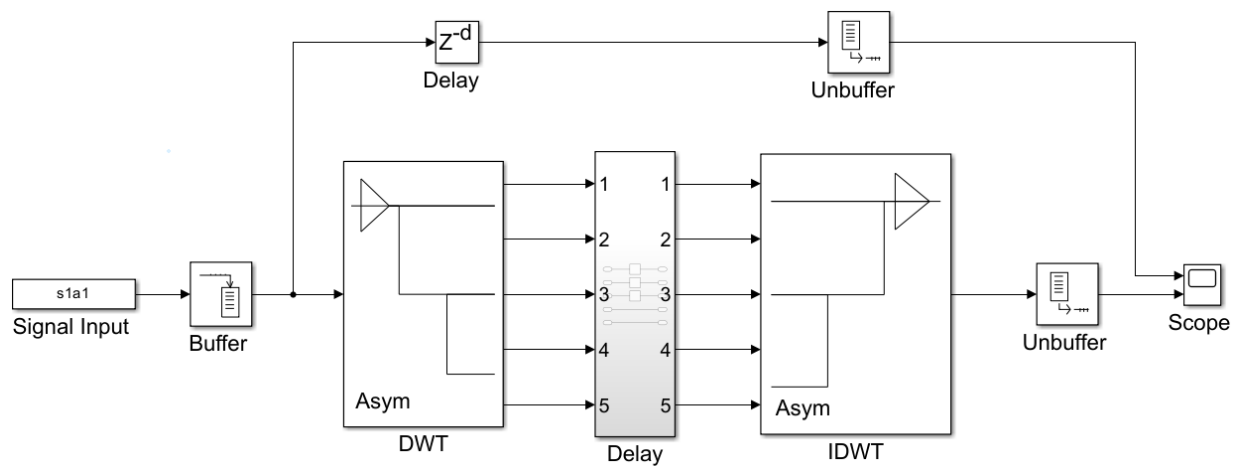


Figure 3.6: sEMG signal processing through the wavelet transform system.

Before signal processing and analysis, data organization was performed, considering the relationship between data and time. First, it is required to open the .mat files to load all the signals in Matlab. Then, run the Matlab script shown in Appendix .2, in which the variables of each signal to be introduced in the “Signal Input” component of the system are set. Finally, in Figure 3.7, it is observed that the initial signal and the signal reconstructed by the wavelet transform are very similar, guaranteeing that the model is functional. It demonstrates that both the choice of the biorthogonal filter 3.5 and the calculation of the delay values were adequate because, with this, it was achieved that the difference between the model and the raw signal was small.

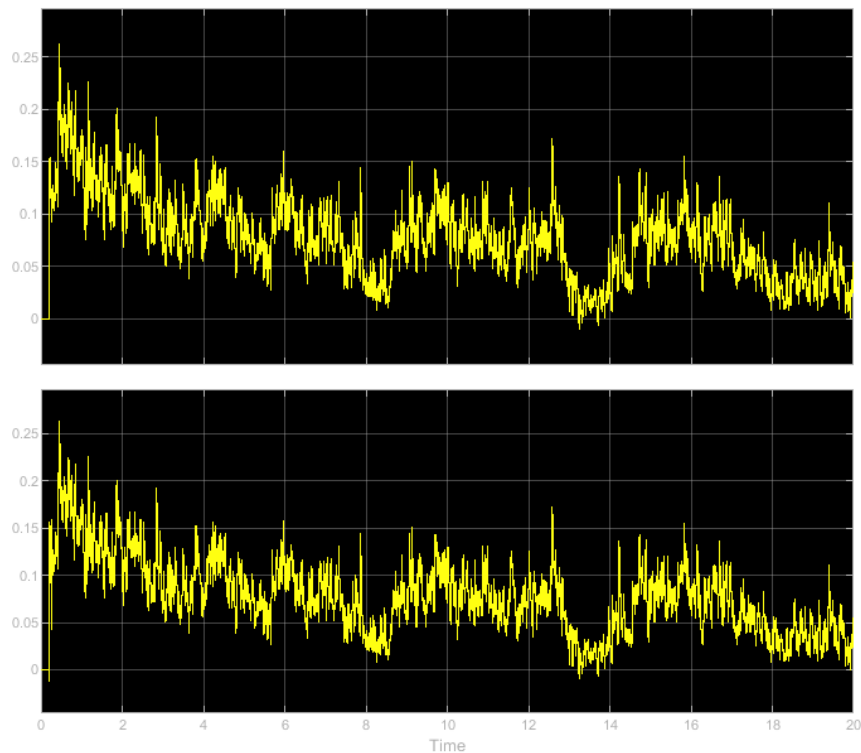


Figure 3.7: Example of a sEMG signal processed using the wavelet transform system.

3.3 sEMG Signal Analysis System

An EMG control system based on pattern recognition includes three components: data segmentation, feature extraction, and classification [88]. Following a literature review, 3 features were selected to analyze the sEMG signals for muscle fatigue detection. The features extracted in the time domain and frequency domain are described below.

- **Mean absolute value:** MAV calculates the absolute values of all signal points and averages them. It represents the average rectified value (ARV) and it is defined by the following equation:

$$MAV = \frac{1}{N} \sum_{i=1}^N |x_i| \quad (3.2)$$

Where X_i is the i^{th} EMG signal and N is the number of samples in each segment [89].

- **Root mean square:** RMS is the square root of the average signal power at a given time. This characteristic quantifies muscle effort. RMS is defined as follows:

$$RMS = \sqrt{\frac{1}{N} \sum_{i=1}^N x_i^2} \quad (3.3)$$

Where N is the length of the window size, and i is the i^{th} sample point [90].

- **Mean Frequency:** MNF is an average frequency value that is computed as a sum of product of the EMG power spectrum and frequency, divided by a total sum of spectrum intensity. It can be expressed as:

$$\text{MNF} = \frac{\sum_{j=1}^N f_j \cdot P_j}{\sum_{j=1}^N P_j} \quad (3.4)$$

Where N is the total number of spectral components, f_j is the frequency corresponding to the j^{th} spectral component, and P_j is the amplitude of the j^{th} spectral component [91].

The MAV, RMS, and MNF are indicators used for fatigue detection in VL [92]. Therefore, a feature extraction subsystem was added to the wavelet system shown above in Section 3.2. Figure 3.8 illustrates the system for feature extraction. Functions were applied to calculate each feature at each DWT decomposition level of the signal before (Figure 3.8a) and after the exercise (Figure 3.8b), the results of which were stored and can be visualized in the final scope of the whole system shown in Figure 3.8c. Moreover, Figure 3.8a and Figure 3.8b show that “Goto” components were also added to send signals to “From” blocks that have the specified tag, and each label was assigned a different color to understand better how these signals are read thanks to the block “Mux” which serves to combine scalar or vector signals of the same type of data and complexity in a virtual vector. In this way, the results of the MAV can be visualized in the system’s final Scope.

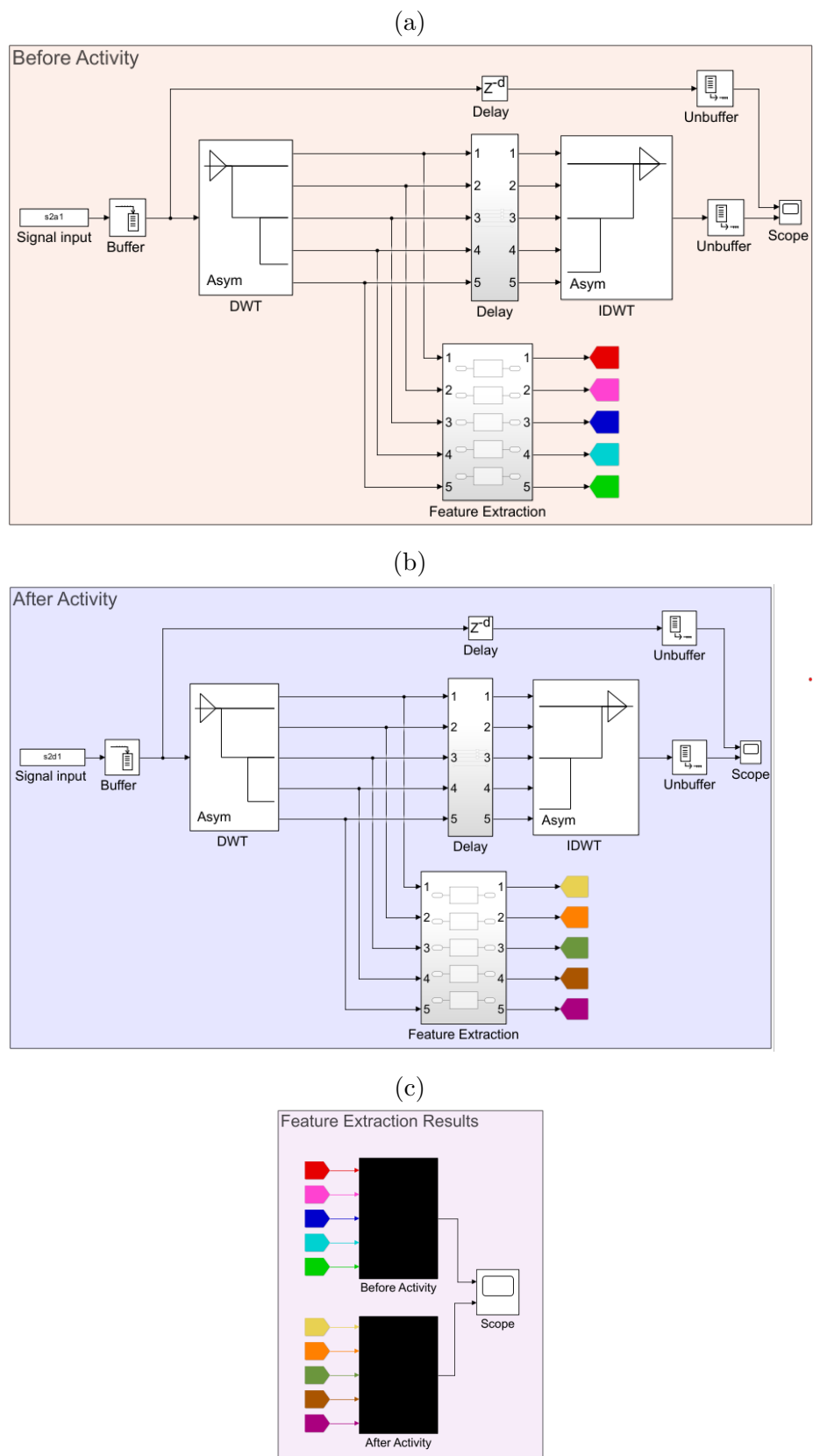


Figure 3.8: Feature extraction system. (a) Before Activity, (b) After Activity, (c) Scope to display.

Additionally, in Figure 3.9, it can be noted that the “Feature Extraction” block/sub-system contains internally an “Input port” component to provide a signal input port, connected to the “MATLAB Function” component in which the function of the feature to be calculated is to be implemented, and an “Output port” component that provides an output port for this subsystem. In addition, in Figure 3.10 are the MAV (Figure 3.10a), RMS (Figure 3.10b), and MNF (Figure 3.10c) functions, implemented in the “MATLAB Function” of the system for each feature, corresponding to the functions 3.2, 3.3, and 3.4, respectively. Alternatively, the “RMS” component provided by the Simulink library could be considered instead of the “MATLAB Function” to calculate this feature. Finally, Figure 3.11 displays an example of the MAV results of each level processed with the DWT of the signal both before (Figure 3.11a), and after (Figure 3.11b) the exercise of one of the participants. These plots can be visualized in the final scope of the feature extraction that we observed in Figure 3.8c, and the same was done for the other two features. As a result, it was confirmed that the last level of DWT decomposition allows the analysis of the different features since it is the one where the signal changes can be best appreciated.

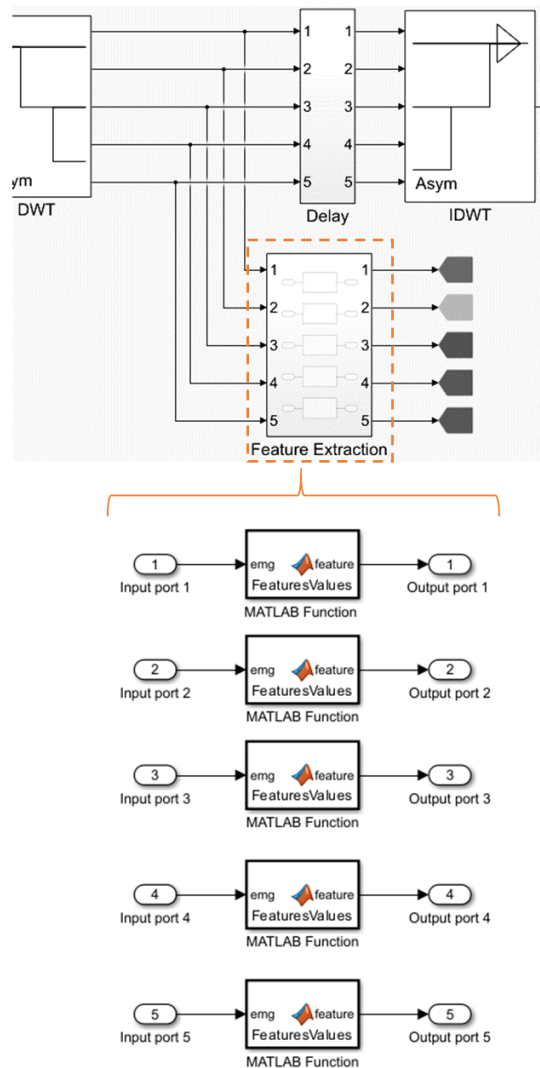


Figure 3.9: Internal content of the ”Feature Extraction” block

(a)

```

filtroWaveAnalysisMAV ▶ Feature Extraction ▶ MATLAB Function
1  function MAV = featuresValues(emg)
2  N = length(emg);
3
4  % ..... MAV .....
5  sumatoria_MAV=0;
6  for n=1:N
7      sumatoria_MAV = sumatoria_MAV+abs(emg(n));
8  end
9
10 MAV = sumatoria_MAV/N;

```

(b)

```

filtroWaveAnalysisRMS ▶ Subsystem ▶ MATLAB Function
1  function RMS = featuresValues(emg)
2  N = length(emg);
3
4  % ..... RMS .....
5  sumatoria_RMS=0;
6  for n=1:N
7      sumatoria_RMS = sumatoria_RMS+(emg(n)^2);
8  end
9
10 RMS = sqrt(sumatoria_RMS/(N));

```

(c)

```

filtroWaveAnalysisMNF ▶ Subsystem ▶ MATLAB Function
1  function MNF = spcAnalysis(emg)
2
3  Fs = 2000;
4  ns = length(emg);
5
6  NFFT = 2^nextpow2(ns);
7  Y = fft(emg,NFFT);
8  f = Fs/2*linspace(0,1,NFFT/2+1);
9  Pe=Y.*conj(Y)/NFFT;
10
11 nf = length(f);
12 np = round(nf/2);
13
14 fout=f(1:np)';
15 Peout=real(Pe(1:NFFT/4+1));
16
17 TTP = sum(Peout);
18
19 if TTP < 0.000000001
20     MNF = 0;
21 else
22     MNF = (fout'*Peout)/TTP;
23 end

```

Figure 3.10: Functions for feature extraction (a) MAV, (b) RMS (c) MNF

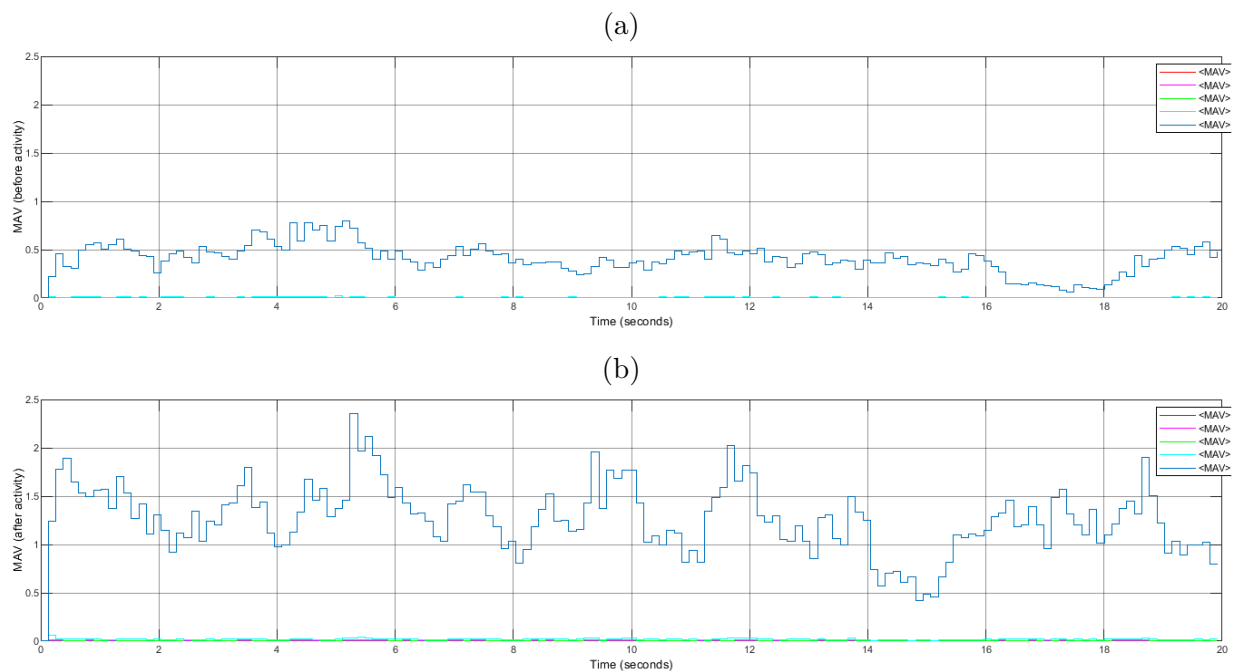


Figure 3.11: Scope of MAV in each level processed with the DWT of participant 2 (first measurement). (a) Before activity, (b) After activity

3.4 Classification Models

Three classification techniques, namely, RF, SVM, and k-NN, were employed to classify fatigue and non-fatigue conditions. For this purpose, Google Colaboratory, also known as “Google Colab” or “Colab”, was used. Google Colab allows to write and execute any Python command or code in the browser, and it is ideal for the creation of ML models [93]. RF is a technique used in several studies, which is based on the construction of multiple decision trees, where each tree grows independently and casts its preference for a class, winning the class with the highest number of votes as a whole [94]. SVM is a supervised ML method, which seeks to find the best classification function to separate classes in training data. It uses a hyperplane in linearly separable cases. SVM ensures finding the optimal solution among an infinite number of possible hyperplanes [61]. k-NN is a classifier algorithm, which determines a set of ‘k’ objects in the training data that is closest to the test object and, using these neighbors, assigns a class to the test object. k-NN consists of three stages: initialization of the dataset and ‘k’ nearest neighbors, calculation of the distance between the neighbors, and classification of the test data according to the most neighboring classes [95]. The script for each classifier model is provided in Appendix .3, Appendix .4, and Appendix .5, and the classification flowchart is illustrated in Figure 3.12. A randomization command was used to split the training set (70%) and the test set (30%) in order to train the three models with the same data. Additionally, for the evaluation of the classification models, sensitivity, specificity, and accuracy were used as performance measures. The mathematical expressions for each of these metrics are given by the equation 3.5, 3.6, and 3.7. Where: TP is true positive, FP is false positive, TN is

true negative, and FN is false negative [96].

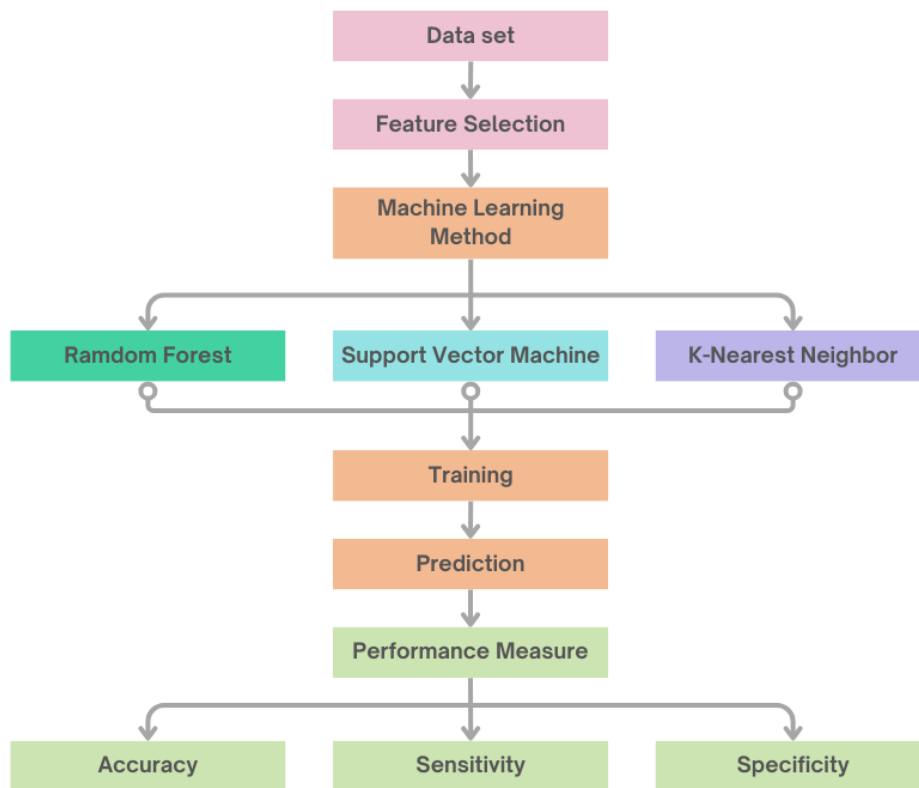


Figure 3.12: Flow chart of the classification models

$$\text{Sensitivity} = \frac{TP}{TP + FN} \quad (3.5)$$

$$\text{Specificity} = \frac{TN}{TN + FP} \quad (3.6)$$

$$\text{Accuracy} = \frac{TP + TN}{TP + TN + FP + FN} \quad (3.7)$$

Chapter 4

Results

In this chapter, it is present the graphical results of the MAV, RMS and MNF extraction of the VL muscle sEMG signals processed with the DWT of one of the participants to show the fatigue patterns present in the signals, as well as a summary table of the analysis of the signals of the 10 participants in the two measurements. The results of the performance parameters of the three trained classification models are also shown. In addition, the raw data can be found at <https://github.com/Marilyn18/sEMG-VL-Data.git>.

4.1 Feature Extraction Analysis

First, in Figure 4.1, the MAV results before (Figure 4.1a) and after (Figure 4.1b) the pre-set exercises of one of the study participants are shown. Overall, in Figure in Figure 4.1a, it was observed to range from 0-0.37 mV, whereas in Figure 4.1b, it increased by about 0-0.81 mV. In addition, higher MAV values were evident in the first 2 seconds of Figure 4.1b compared to Figure 4.1a. In Figure 4.1b, it was also visualized that in the second 6.7, the highest MAV peak was pronounced, being 0.81 mV, while in Figure 4.1a its value was 0.27 mV. Furthermore, between 8-10 seconds, high peaks were also noted in Figure 4.1b of 0.78 and 0.75 mV, and another large increase in the MAV peak was pronounced in the range of 14.6 to 15.8 seconds when the values ranged from 0.58 to 0.74 mV. Finally, from second 16 to 20, a drop in the intensity of the MAV values was noted (Figure 4.1b); however, they are still higher values when compared to those calculated in Figure 4.1a. Therefore, it was determined that the person is fatigued from the increase in MAV.

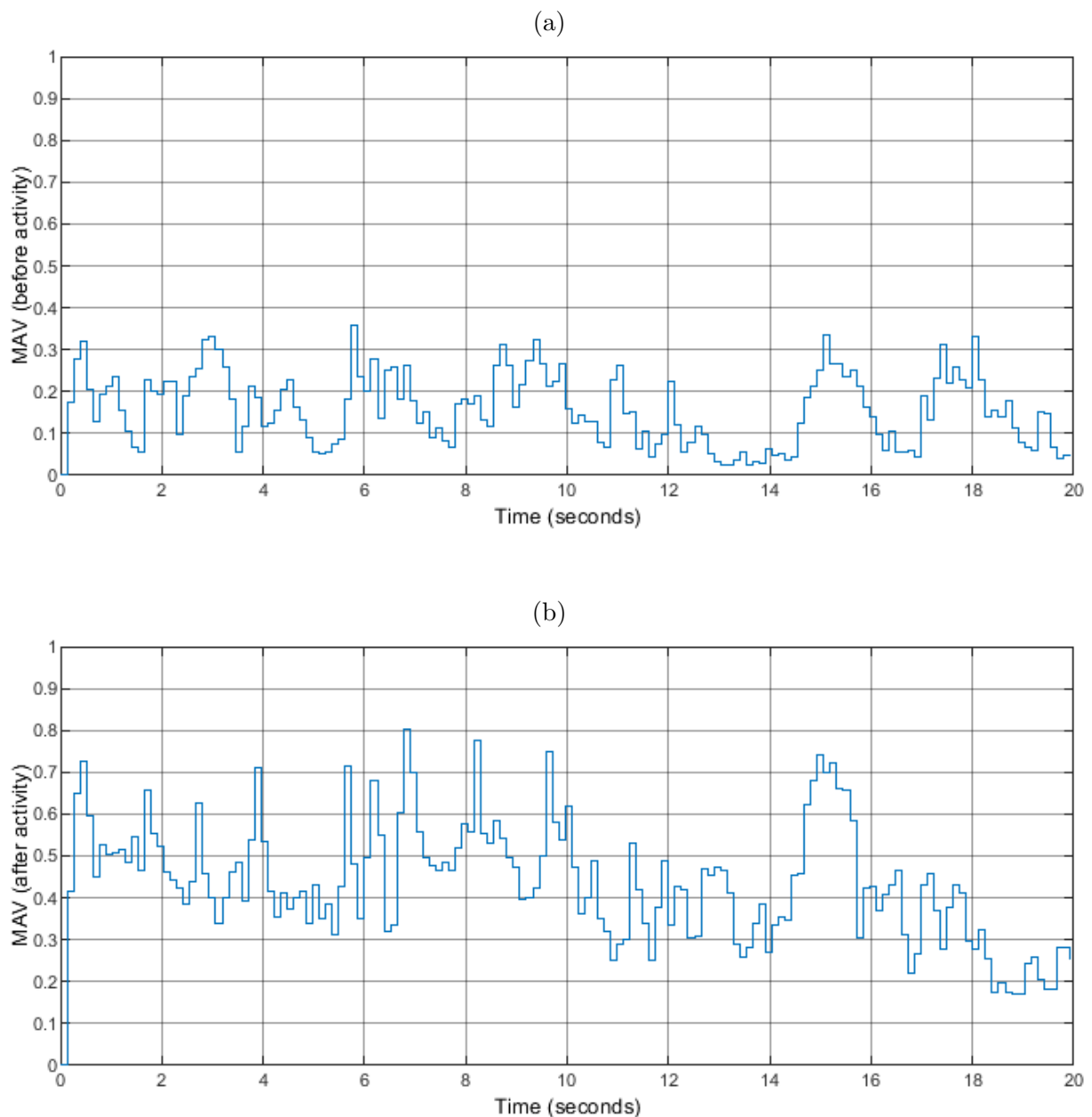


Figure 4.1: Mean Absolute Value of the participant 4 (first measurement). (a) Before activity, (b) After activity.

Secondly, Figure 4.2 shows the RMS results before (Figure 4.2a) and after (Figure 4.2b) the participant's activity. In Figure 4.2a, the RMS ranges from 0 to 0.37 mV, and in Figure 4.2b, it increases to 0.81 mV. Furthermore, in Figure 4.2b, the highest peaks occurred around 0.7-4 s, 5.5-10 s, and 14-16 s, with RMS values similar to those of the MAV shown in the previous figure (Figure 4.1b). In Figure 4.2b, it was noted that the highest point was 0.81 mV at 6.7 s, and although the RMS from second 16 to 20 decreased a little, its values hovered around 0.16-0.47 mV, while in Figure 4.2a it hovered between 0.05-0.33 mV. That is, RMS also presented an increasing trend in the presence of fatigue. Thirdly, Figure 4.3 shows the MNF results before (Figure 4.3a) and after (Figure 4.3b) the activity. In Figure

4.3a, the MNF reached approx 114 Hz, while in Figure 4.3b, the maximum value of the MNF was 23 Hz, that is its highest peak at second 0.1, which coincides with the same value of MNF at second 0.1 in Figure 4.3a. In other words, there was no increase in MNF after exercise at any time, and there was a significant decrease in MNF as an indicator of muscle fatigue. Finally, the analysis results of the characteristics extraction of all participants are summarized in Table 4.1, where NSC (no significant change) means that the results before and after exercise were in the same range or with non-significant increases and decreases.

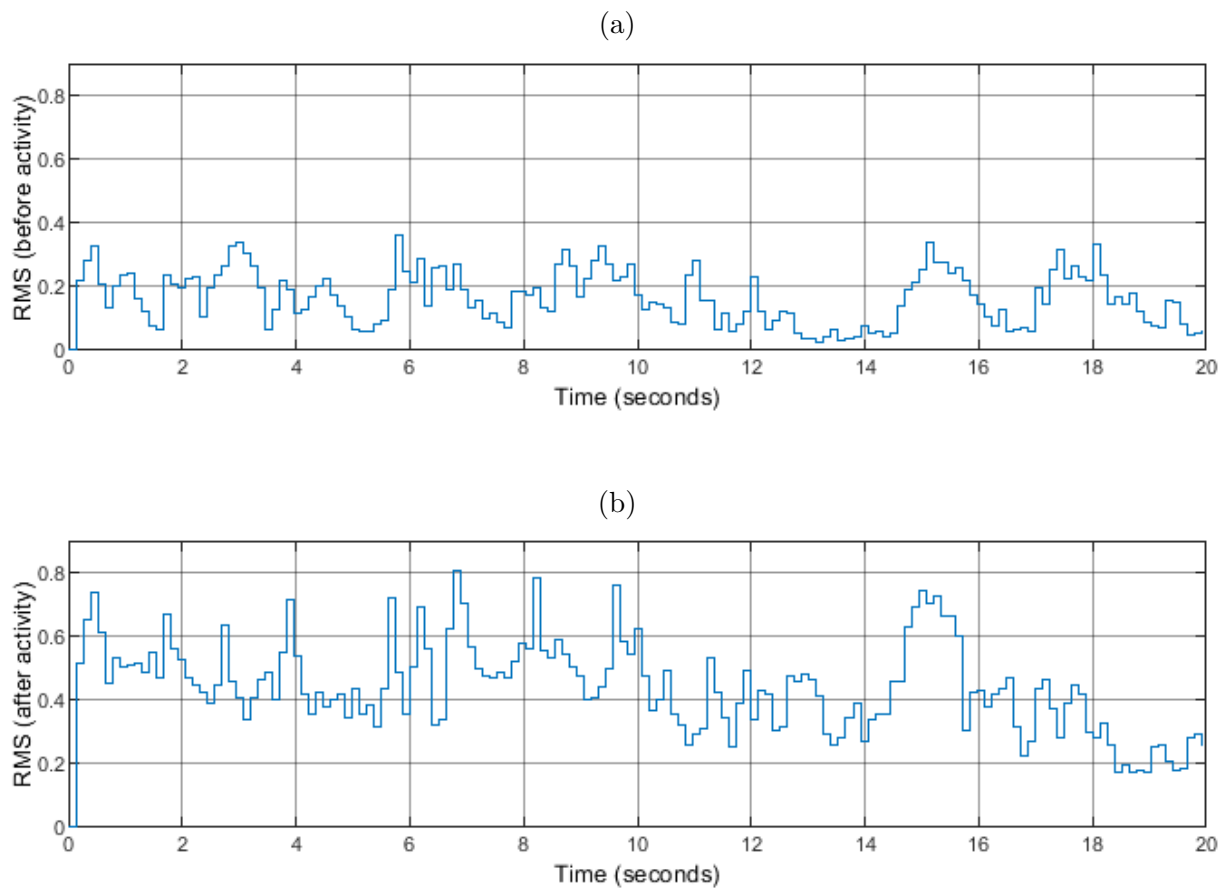


Figure 4.2: Root Mean Square of the participant 4 (first measurement). (a) Before activity, (b) After activity.

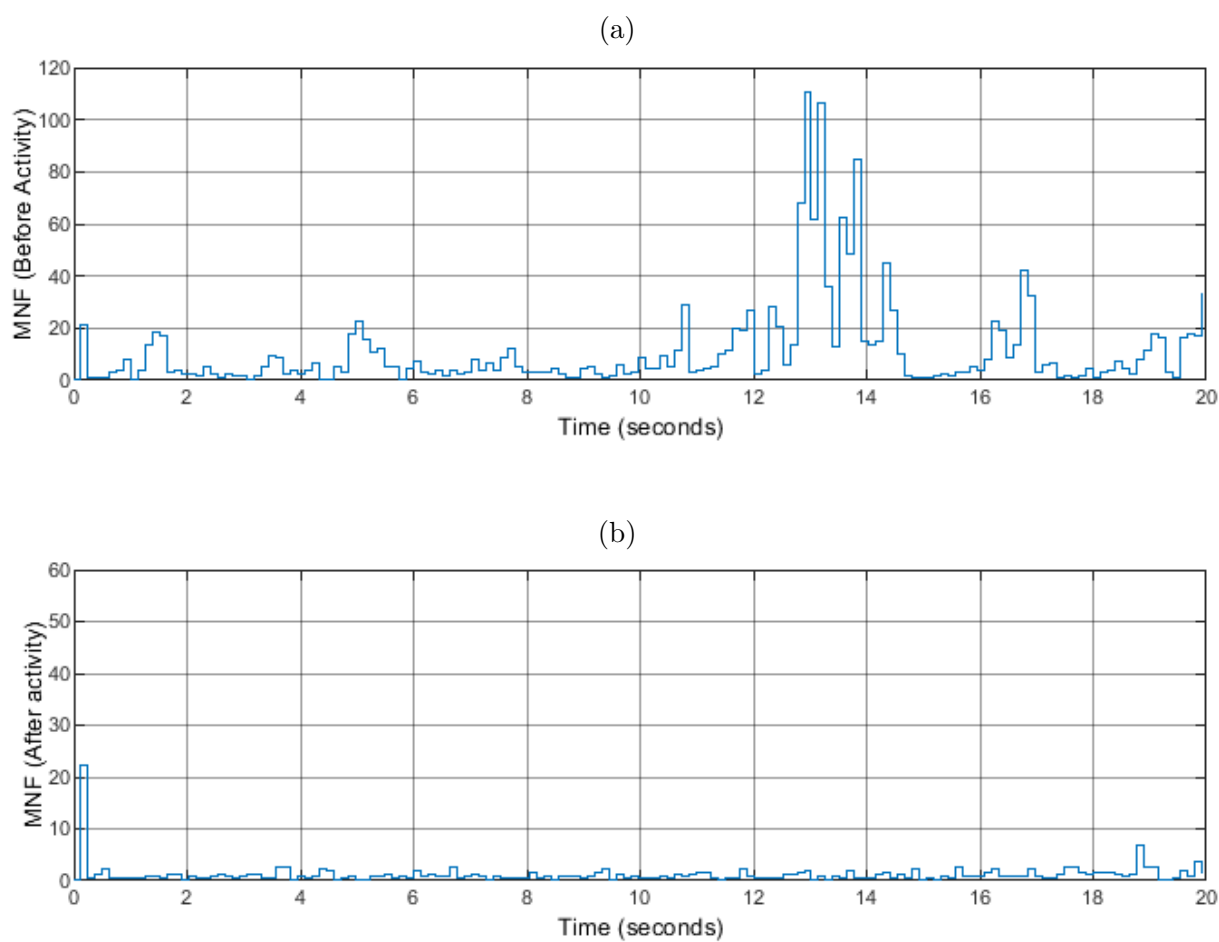


Figure 4.3: Mean Frequency of the participant 4 (first measurement). (a) Before activity, (b) After activity.

Table 4.1: Summary of feature extraction analysis.

P	Measure	MAV	RMS	MNF	Classification
1	1	NSC	NSC	NSC	Non-Fatigue
	2	Increase	Increase	Decrease	Fatigue
2	1	Increase	Increase	Decrease	Fatigue
	2	Increase	Increase	Decrease	Fatigue
3	1	NSC	NSC	NSC	Non-Fatigue
	2	Increase	Increase	Decrease	Fatigue
4	1	Increase	Increase	Decrease	Fatigue
	2	Increase	Increase	Decrease	Fatigue
5	1	Increase	Increase	Decrease	Fatigue
	2	Increase	Increase	Decrease	Fatigue
6	1	NSC	NSC	Decrease	Non-Fatigue
	2	Increase	Increase	Decrease	Fatigue
7	1	Increase	Increase	Decrease	Fatigue
	2	Increase	Increase	Decrease	Fatigue
8	1	NSC	NSC	NSC	Non-Fatigue
	2	Increase	Increase	Decrease	Fatigue
9	1	Increase	Increase	Decrease	Fatigue
	2	Increase	Increase	Decrease	Fatigue
10	1	NSC	Increase	NSC	Non-Fatigue
	2	NSC	NSC	NSC	Non-Fatigue

4.2 Classifier Models Performance

It was found that the RF model exhibited remarkable efficiency in classifying fatigue and non-fatigue conditions based on features extracted from VL sEMG signals, such as MAV, RMS and MNF. Specifically, RF achieved a sensitivity, specificity and accuracy of 100%. On the other hand, the SVM and k-NN models showed comparable results in terms of sensitivity, specificity and accuracy, with values of 50%, 75% and 83.33%, respectively. Both these models proved to be equally competent in classifying fatigue and non-fatigue conditions, using the characteristics of VL sEMG signals during isometric contractions after gym exercise sessions.

Table 4.2: Classification performance of the extracted features for muscle fatigue detection.

Classifier	Sensitivity (%)	Specificity (%)	Accuracy (%)
SVM	50	75	83.33
k-NN	50	75	83.33
RF	100	100	100

Chapter 5

Discussion

The MAV; RMS, and MNF results of a specific participant were shown as a general example because the same pattern was observed in the signal analysis of most of the participants. In addition, feature extraction plays an essential role in increasing the accuracy of classification since the effectiveness of the classifiers depends on the adequate information provided to them [97]. Participants 1, 3, 6, and 8 did not show fatigue in the first measurement performed, which shows that they did not exceed their resistance limit [98]. However, these participants increased the weight in the exercises performed on the second day of measurements, and this time, they did show fatigue. On the other hand, participant 10 did not present fatigue in either the first or the second measurement. It is important to mention that participants 6, 8, and 10 are women. In the literature, it is mentioned that women are less prone to suffer muscle fatigue because they have a greater endurance [99] and have a higher content of type I muscle fibers (slow twitch fibers) compared to men [100]. Moreover, fatigue is likely to be linked to muscle mass, which theoretically influences oxygen demand and perfusion during muscle contractions at the same relative strength level [101].

The most commonly used method for the analysis of sEMG signals is DWT due to the ability of the wavelets to adjust the temporal resolution individually for each frequency. This means that it provides a higher time result for high bands and a lower resolution time for low-frequency bands. In contrast, the Fourier Transform maintains the same resolution for each band, resulting in a less accurate approximation in both time and frequency of physiological signals [102]. In addition, DWT is known to provide sufficient information about the signal, with a great improvement in computation time compared to STFT [103]. Based on the results of the present work, it is evident that the use of the DWT for the raw signal processing and the extraction of time domain and frequency domain characteristics allowed to obtain the expected results for fatigue detection based on the literature. In fact, it is known that two common indicators used to measure and analyze the amplitude of the sEMG in modern digital systems are the MAV and RMS [30] [104]. The results obtained in this study evidenced an increasing trend in the MAV and RMS after exercise in most of the participants. Another study in which they analyzed the sEMG of the rectus femoris muscle in static contractions showed an increase in MAV, frequency shift in the power spectrum towards lower frequencies, and increase in the amplitude and duration of an averaged action potential of the motor unit as part of the changes in the signal as a

result of fatigue [105]. This suggests a general increase in the signal amplitude measured over time. In a different study, they performed simultaneous measurements of myoelectric signals both within the muscles and at the muscle surface, and the results showed that fatigue increased the RMS of the surface myoelectric signal [106]. This is due to the frequency shift of the power spectrum towards lower frequencies. The tissue has the property of attenuating or reducing the higher frequencies of the electrical signals, like a low-pass filter, allowing more energy to reach the surface electrodes [107]. In addition, the results obtained in the present study of MAV and RMS were very similar. The same happened in another study [108], where they also mentioned that the MAV feature, from the point of view of class separability, is better than the RMS, so they only discussed the MAV results. Furthermore, the decreasing trend in the MNF after exercise was also observed in most of the participants. MNF has proven to be useful in identifying alterations in the frequency and patterns of MUs recruitment that are produced by metabolic changes during muscle fatigue [109]. Some researches mentioned using sEMG to assess VL muscle fatigability under isometric conditions, the shift of MNF towards lower frequencies was considered [43]. MNF is commonly used in sEMG analysis to assess muscle fatigue. When a muscle is fatigued, the frequency of action potentials generated by the motor units decreases, which is reflected in a shift towards lower frequencies in the sEMG frequency spectrum. Besides, sEMG power spectrum analysis is a valuable tool for detecting muscle fatigue, and it is enhanced by combining this analysis with time domain features to consider more information about the muscles and avoid missing information [10]. In general terms, the literature has confirmed that an increase in MAV and RMS in the time domain, as well as a decrease in MNF in the frequency domain, are indicators of muscle fatigue [92] [102]. According to Abdelouahad et al., [7], the increase in MAV and RMS during muscle contraction is also related to the increase in force level contraction. Moreover, Belkacem et al. [110] added that MNF, in addition to MAV and RMS, is also influenced by both the level of produced maximum voluntary contraction and fatigue. However, when comparing the signal measurements before and after exercise in the present study, it was noted that the alterations presented in the analysis of the extracted characteristics occurred after physical activity, so it is associated with fatigue.

Among the traditional ML algorithms used, the RF model showed better performance than the SVM, and the k-NN for fatigue classification. Zhang et al. [69] also used these three techniques in their study to evaluate the performance, and similarly found that RF obtained better accuracy than SVM and k-NN. Although traditional ML methods can present some problems in certain cases [64] and be challenging for complex EMG signals [111], they are the most recommended when dealing with small datasets [2]. In this work, the RF achieved "perfect" performance, which is due to the overtraining factor. The overfitting or overtraining effect of a model can happen when the training dataset is small, and when the training data (features) are too optimistic/good [112]. Sensitivity is the ability (of the classifier) to produce a positive result for a person with the condition of interest (fatigue), while specificity reflects the ability to produce a negative result for a person without the condition (non-fatigue) [113]. Although all three models were trained with the same data set, RF provided perfect sensitivity, specificity, and accuracy, whereas in the SVM and k-NN models these decreased. This indicates that RF could be an effective technique for muscle fatigue classification. However, these findings serve as a basis for future

research to further investigate its effectiveness and performance, expanding the data and perhaps increasing the number of characteristics analyzed.

The effectiveness of the method proposed in this work for the analysis of sEMG signals in the VL for the detection of muscle fatigue is a useful tool for monitoring neuromuscular performance and creating training strategies for young athletes to prevent overtraining and injuries. On one hand, overtraining syndrome is a condition that occurs due to intense and excessive training [114] and it is characterized by persistent fatigue, low athletic performance, changes in mood, among other factors. Having an early indicator to prevent overtraining before serious symptoms occur is a necessity for an athlete's career, as well as having a training program that includes regular monitoring to assess short and long-term adaptation to training [115]. On the other hand, neuromuscular performance plays a significant role in patellar dislocations, suggesting implications for knee injury prevention. Patellar dislocation is a common injury in the patellofemoral joint, especially in young athletes. Its treatment can vary from conservative approaches, such as physiotherapy and rest, to more invasive surgical interventions, such as patellofemoral ligament reconstruction, patellar realignment, repair of damaged cartilage, etc. Additionally, postoperative rehabilitation is required to ensure optimal recovery [116]. Therefore, this work contributes to the field of sports performance and injury prevention because it has been reported that the use of a muscle fatigue detection system could help prevent injuries caused by overexertion [102]. Finally, this work presented some limitations such as having a small database, which produced a performance of 100% of the RF, and a low sensitivity of 50% and specificity of 75% of the SVM and k-NN. Another limitation, as also mentioned by Zhang et al. [69], was the lack of a uniform measure of muscle fatigue. To overcome this problem, standardization of muscle fatigue measurements is required to improve the accuracy and reliability of fatigue detection methods based on sEMG signals. The literature, however, has not yet reached a consensus on these values because they are directly related to each individual and task [117].

Chapter 6

Conclusions

- Measurements of sEMG signals on the VL muscle were performed before and after the conduction of exercises in the gym in a group of 10 participants, by following the specific skin preparation guidelines and adequate placement of the surface electrodes. This procedure allowed to obtain the database to carry out an analysis of the signal for the muscle fatigue detection.
- A system for the signal processing was designed in Simulink by implementing the DWT, a bior 3.5 filter, level 4, and asymmetric structure. The signals were reconstructed by attenuating the noise, and keeping the relevant information of the signal. This was verified since the difference between the model result values and the initial signal values was small. Moreover, the signal decomposition using the DWT made it possible to analyze the variations in muscle activity by extracting characteristics from the time domain and the frequency domain.
- The obtention of MAV, RMS, and MNF of the sEMG signal was achieved before and after the exercises, and the results of both were compared to identify any pattern associated to the muscle fatigue. Results prove that MAV and RMS increases, whilst the MNF decreases, when there is muscle fatigue. These results also confirm the importance of features extraction for the muscle condition evaluation.
- The results of the model proposed in the present work were validated by comparing them with those in the literature. The results clearly showed that the parameters in the time domain increase and the parameters in the frequency domain decrease in the fatigue state. Additionally, the analysis allowed the application of the traditional ML models of classification RF, SVM, and k-NN, which reached an accuracy of 100%, 83.33%, and 83.33%, respectively.
- The present work presented a non-invasive and efficient method for the analysis of sEMG signals for the detection of muscle fatigue and the optimization of physical performance. These findings have important implications for clinical and sports practice, as they provide an effective methodology for assessing muscle condition, which allows the creation of training strategies to prevent injuries.

6.1 Recommendations

- It is essential to consider the external elements that can trigger interferences in the signal, such as interferences caused by the movement of the participant, or the movement of the cables, so we can avoid them. This will help to minimize the noise added to the signals, thus improving the quality of the data obtained.
- Provide the participants with an explanation of the procedure to be followed during the data collection, in order to avoid possible delays and allow a more efficient and accurate execution of the required activities.
- The use of personal and unique electrodes for each individual during sEMG signal measurements is highly recommended.
- It is critical to ensure the correct handling and use of the materials utilized in signal acquisition, in order to prevent damage that could compromise the integrity of the equipment and the accuracy of the measurements.
- Keep the batteries of the equipment properly charged before each measurement session, in order to ensure optimal performance, avoid interruptions during the data acquisition process, and guarantee the reliability of the measurements.
- Keep the computer used in the signal acquisition process always with battery charge, in order to avoid possible interruptions in the data recording due to sudden power outages. This will ensure data integrity and continuity of the signal acquisition process.
- Check that the signal has been correctly recorded before saving it. This will ensure the integrity of the stored data for further processing and analysis.

6.2 Future works

- To apply the system designed in this work for the detection of muscle fatigue in the other muscles of the lower body, such as the rectus femoris, and vastus medialis.
- Expand the database with a larger number of participants to develop a more solid database in order to train a neural network for the automatic detection of muscle fatigue.
- To carry out an exhaustive study of muscle fatigue detection in athletes of various sports disciplines, such as soccer, basketball, cycling, running and gym training. This comparative analysis will permit to determine which type of exercise is most linked to the onset and development of muscle fatigue.
- Conduct a complementary investigation using the same methodology for the muscle fatigue detection, but focusing on the measurement of sEMG signals during dynamic contractions. This approach will provide a more detailed understanding of muscle fatigue patterns in different physical activities.

Bibliography

- [1] P. Konrad, “The abc of emg,” *A practical introduction to kinesiological electromyography*, vol. 1, no. 2005, pp. 30–5, 2005.
- [2] R. I. Mukhamediev, A. Symagulov, Y. Kuchin, K. Yakunin, and M. Yelis, “From classical machine learning to deep neural networks: A simplified scientometric review,” *Applied Sciences*, vol. 11, no. 12, p. 5541, 2021.
- [3] W. Wilson, “Wavelet analysis for audiologists,” *Australian and New Zealand Journal of Audiology, The*, vol. 24, no. 2, pp. 92–104, 2002.
- [4] M. Li, J. Li, and M. Shu, “Detection of muscle fatigue by fusion of agonist and synergistic muscle semg signals,” in *2020 IEEE 33rd International Symposium on Computer-Based Medical Systems (CBMS)*. IEEE, 2020, pp. 95–98.
- [5] H. Piper, *Elektrophysiologie menschlicher muskeln*. Springer, 1912.
- [6] M. González-Izal, A. Malanda, E. Gorostiaga, and M. Izquierdo, “Electromyographic models to assess muscle fatigue,” *Journal of Electromyography and Kinesiology*, vol. 22, no. 4, pp. 501–512, 2012.
- [7] A. Abdelouahad, A. Belkhou, A. Jbari, and L. Bellarbi, “Time and frequency parameters of semg signal—force relationship,” in *2018 4th International Conference on Optimization and Applications (ICOA)*. IEEE, 2018, pp. 1–5.
- [8] D. Mu, F. Li, L. Yu, C. Du, L. Ge, and T. Sun, “Study on exercise muscle fatigue based on semg and ecg data fusion and temporal convolutional network,” *Plos one*, vol. 17, no. 12, p. e0276921, 2022.
- [9] R. Merletti, A. Botter, A. Troiano, E. Merlo, and M. A. Minetto, “Technology and instrumentation for detection and conditioning of the surface electromyographic signal: state of the art,” *Clinical biomechanics*, vol. 24, no. 2, pp. 122–134, 2009.
- [10] H. A. Yousif, A. Zakaria, N. A. Rahim, A. F. B. Salleh, M. Mahmood, K. A. Alfarhan, L. M. Kamarudin, S. M. Mamduh, A. M. Hasan, and M. K. Hussain, “Assessment of muscles fatigue based on surface emg signals using machine learning and statistical approaches: A review,” in *IOP conference series: materials science and engineering*, vol. 705, no. 1. IOP Publishing, 2019, p. 012010.
- [11] J. Wang, S. Sun, and Y. Sun, “A muscle fatigue classification model based on lstm and improved wavelet packet threshold,” *Sensors*, vol. 21, no. 19, p. 6369, 2021.

- [12] T. T. Zawawi, A. R. Abdullah, E. F. Shair, I. Halim, and O. Rawaida, "Electromyography signal analysis using spectrogram," in *2013 IEEE Student Conference on Research and Development*. IEEE, 2013, pp. 319–324.
- [13] M. G. Jahromi, H. Parsaei, A. Zamani, and M. Dehbozorgi, "Comparative analysis of wavelet-based feature extraction for intramuscular emg signal decomposition," *Journal of biomedical physics & engineering*, vol. 7, no. 4, p. 365, 2017.
- [14] R. Merletti and P. J. Parker, *Electromyography: physiology, engineering, and non-invasive applications*. John Wiley & Sons, 2004, vol. 11.
- [15] C. Disselhorst-Klug, T. Schmitz-Rode, and G. Rau, "Surface electromyography and muscle force: Limits in semg–force relationship and new approaches for applications," *Clinical biomechanics*, vol. 24, no. 3, pp. 225–235, 2009.
- [16] S. Day, "Important factors in surface emg measurement," *Bortec Biomedical Ltd publishers*, pp. 1–17, 2002.
- [17] C. J. De Luca, A. Adam, R. Wotiz, L. D. Gilmore, and S. H. Nawab, "Decomposition of surface emg signals," *Journal of neurophysiology*, vol. 96, no. 3, pp. 1646–1657, 2006.
- [18] C. J. De Luca, L. D. Gilmore, M. Kuznetsov, and S. H. Roy, "Filtering the surface emg signal: Movement artifact and baseline noise contamination," *Journal of biomechanics*, vol. 43, no. 8, pp. 1573–1579, 2010.
- [19] C. Tepe and M. C. Demir, "The effects of the number of channels and gyroscopic data on the classification performance in emg data acquired by myo armband," *Journal of Computational Science*, vol. 51, p. 101348, 2021.
- [20] T. Lulic-Kuryllo, F. Negro, N. Jiang, and C. R. Dickerson, "Standard bipolar surface emg estimations mischaracterize pectoralis major activity in commonly performed tasks," *Journal of Electromyography and Kinesiology*, vol. 56, p. 102509, 2021.
- [21] J. Correa-Figueroa, E. Morales-Sánchez, J. Huerta-Ruelas, J. González-Barbosa, and C. Cárdenas-Pérez, "Sistema de adquisición de señales semg para la detección de fatiga muscular," *Revista mexicana de ingeniería biomédica*, vol. 37, no. 1, pp. 17–27, 2016.
- [22] A. Del Vecchio, A. Holobar, D. Falla, F. Felici, R. Enoka, and D. Farina, "Tutorial: Analysis of motor unit discharge characteristics from high-density surface emg signals," *Journal of Electromyography and Kinesiology*, vol. 53, p. 102426, 2020.
- [23] B. S. Darak and S. Hambarde, "A review of techniques for extraction of cardiac artifacts in surface emg signals and results for simulation of ecg-emg mixture signal," in *2015 International conference on pervasive computing (ICPC)*. IEEE, 2015, pp. 1–5.
- [24] S. Pourmohammadi and A. Maleki, "Stress detection using ecg and emg signals: A comprehensive study," *Computer methods and programs in biomedicine*, vol. 193, p. 105482, 2020.

- [25] L. Xu, X. Chen, S. Cao, X. Zhang, and X. Chen, "Feasibility study of advanced neural networks applied to semg-based force estimation," *Sensors*, vol. 18, no. 10, p. 3226, 2018.
- [26] A. M. Khan, S. G. Khawaja, M. U. Akram, and A. S. Khan, "semg dataset of routine activities," *Data in brief*, vol. 33, p. 106543, 2020.
- [27] K.-M. Chang, S.-H. Liu, and X.-H. Wu, "A wireless semg recording system and its application to muscle fatigue detection," *Sensors*, vol. 12, no. 1, pp. 489–499, 2012.
- [28] F. Di Nardo, C. Morbidoni, A. Cucchiarelli, and S. Fioretti, "Influence of emg-signal processing and experimental set-up on prediction of gait events by neural network," *Biomedical Signal Processing and Control*, vol. 63, p. 102232, 2021.
- [29] M. B. I. Reaz, M. S. Hussain, and F. Mohd-Yasin, "Techniques of emg signal analysis: detection, processing, classification and applications," *Biological procedures online*, vol. 8, pp. 11–35, 2006.
- [30] M. Cifrek, V. Medved, S. Tonković, and S. Ostojić, "Surface emg based muscle fatigue evaluation in biomechanics," *Clinical biomechanics*, vol. 24, no. 4, pp. 327–340, 2009.
- [31] R. M. Enoka and J. Duchateau, "Muscle fatigue: what, why and how it influences muscle function," *The Journal of physiology*, vol. 586, no. 1, pp. 11–23, 2008.
- [32] M. R. Al-Mulla, F. Sepulveda, and M. Colley, "A review of non-invasive techniques to detect and predict localised muscle fatigue," *Sensors*, vol. 11, no. 4, pp. 3545–3594, 2011.
- [33] B. K. Barry and R. M. Enoka, "The neurobiology of muscle fatigue: 15 years later," *Integrative and comparative biology*, vol. 47, no. 4, pp. 465–473, 2007.
- [34] V. J. Gawron, J. French, and D. Funke, "An overview of fatigue," *Stress, workload, and fatigue*, pp. 581–595, 2000.
- [35] C. Froyd, F. G. Beltrami, G. Y. Millet, and T. D. Noakes, "Central regulation and neuromuscular fatigue during exercise of different durations," *Med Sci Sports Exerc*, vol. 48, no. 6, pp. 1024–32, 2016.
- [36] H. Tankisi, D. Burke, L. Cui, M. de Carvalho, S. Kuwabara, S. D. Nandedkar, S. Rutkove, E. Stålberg, M. J. van Putten, and A. Fuglsang-Frederiksen, "Standards of instrumentation of emg," *Clinical neurophysiology*, vol. 131, no. 1, pp. 243–258, 2020.
- [37] J. G. Webster, "Amplifiers and signal processing," *Medical instrumentation: application and design*, vol. 4, 1998.
- [38] L. R. Robinson, M. Christie, and S. Nandedkar, "A message from the ground electrode," *Muscle & nerve*, vol. 54, no. 6, pp. 1010–1011, 2016.

- [39] S. D. Nandedkar and P. E. Barkhaus, “Defective e2 electrode lead gives low-amplitude compound muscle action potential,” *Muscle & Nerve*, vol. 67, no. 4, pp. 310–314, 2023.
- [40] M. J. A. M. van Putten, *Essentials of neurophysiology: basic concepts and clinical applications for scientists and engineers*. Springer, 2009.
- [41] R. H. Chowdhury, M. B. Reaz, M. A. B. M. Ali, A. A. Bakar, K. Chellappan, and T. G. Chang, “Surface electromyography signal processing and classification techniques,” *Sensors*, vol. 13, no. 9, pp. 12 431–12 466, 2013.
- [42] B. FENGJUN, “Muscle force estimation and fatigue detection based on semg signals,” 2013.
- [43] Ü. Kaljumäe, O. Hänninen, and O. Airaksinen, “Knee extensor fatigability and strength after bicycle ergometer training,” *Archives of physical medicine and rehabilitation*, vol. 75, no. 5, pp. 564–567, 1994.
- [44] M. Knaflitz and P. Bonato, “Time-frequency methods applied to muscle fatigue assessment during dynamic contractions,” *Journal of Electromyography and Kinesiology*, vol. 9, no. 5, pp. 337–350, 1999.
- [45] L. Cohen, *Time-frequency analysis*. Prentice Hall PTR Englewood Cliffs, 1995, vol. 778.
- [46] P. Coorevits, L. Danneels, D. Cambier, H. Ramon, H. Druyts, J. S. Karlsson, G. De Moor, and G. Vanderstraeten, “Correlations between short-time fourier-and continuous wavelet transforms in the analysis of localized back and hip muscle fatigue during isometric contractions,” *Journal of Electromyography and Kinesiology*, vol. 18, no. 4, pp. 637–644, 2008.
- [47] J. Duchene, D. Devedeux, S. Mansour, and C. Marque, “Analyzing uterine emg: tracking instantaneous burst frequency,” *IEEE Engineering in Medicine and Biology Magazine*, vol. 14, no. 2, pp. 125–132, 1995.
- [48] Q. Tan, Y. Wang, T. L.-W. Chen, D. W.-C. Wong, F. Yan, Z. Li, and M. Zhang, “Exercise-induced hemodynamic changes in muscle tissue: Implication of muscle fatigue,” *Applied Sciences*, vol. 10, no. 10, p. 3512, 2020.
- [49] A. Abbate, C. DeCusatis, and P. K. Das, *Wavelets and subbands: fundamentals and applications*. Springer Science & Business Media, 2012.
- [50] J. Karlsson, B. Gerdle, and M. Akay, “Analyzing surface myoelectric signals recorded during isokinetic contractions,” *IEEE Engineering in Medicine and Biology Magazine*, vol. 20, no. 6, pp. 97–105, 2001.
- [51] S. Karlsson, J. Yu, and M. Akay, “Time-frequency analysis of myoelectric signals during dynamic contractions: a comparative study,” *IEEE transactions on Biomedical Engineering*, vol. 47, no. 2, pp. 228–238, 2000.

- [52] J.-Y. Kim, M.-C. Jung, and J. M. Haight, "The sensitivity of autoregressive model coefficient in quantification of trunk muscle fatigue during a sustained isometric contraction," *International Journal of Industrial Ergonomics*, vol. 35, no. 4, pp. 321–330, 2005.
- [53] D. Moshou, I. Hostens, G. Papaioannou, and H. Ramon, "Dynamic muscle fatigue detection using self-organizing maps," *Applied soft computing*, vol. 5, no. 4, pp. 391–398, 2005.
- [54] R. Boostani and M. H. Moradi, "Evaluation of the forearm emg signal features for the control of a prosthetic hand," *Physiological measurement*, vol. 24, no. 2, p. 309, 2003.
- [55] G. Zhang, E. Morin, Y. Zhang, and S. A. Etemad, "Non-invasive detection of low-level muscle fatigue using surface emg with wavelet decomposition," in *2018 40th annual international conference of the ieee engineering in medicine and biology society (embc)*. IEEE, 2018, pp. 5648–5651.
- [56] V. Bonilla *et al.*, "Study of noise and interference of surface electromyography signal and wavelet denoising," , no. 2-3 (7), pp. 32–36, 2015.
- [57] "Artificial intelligence," <https://www.britannica.com/technology/artificial-intelligence>.
- [58] G. Nguyen, S. Dlugolinsky, M. Bobák, V. Tran, Á. López García, I. Heredia, P. Malík, and L. Hluchý, "Machine learning and deep learning frameworks and libraries for large-scale data mining: a survey," *Artificial Intelligence Review*, vol. 52, pp. 77–124, 2019.
- [59] J. Wang, Y. Sun, and S. Sun, "Recognition of muscle fatigue status based on improved wavelet threshold and cnn-svm," *IEEE Access*, vol. 8, pp. 207 914–207 922, 2020.
- [60] Q. Liu, Y. Liu, C. Zhang, Z. Ruan, W. Meng, Y. Cai, and Q. Ai, "semg-based dynamic muscle fatigue classification using svm with improved whale optimization algorithm," *IEEE Internet of Things Journal*, vol. 8, no. 23, pp. 16 835–16 844, 2021.
- [61] G. Venugopal, M. Navaneethakrishna, and S. Ramakrishnan, "Extraction and analysis of multiple time window features associated with muscle fatigue conditions using semg signals," *Expert Systems with Applications*, vol. 41, no. 6, pp. 2652–2659, 2014.
- [62] G. Venugopal and S. Ramakrishnan, "Differentiating semg signals under muscle fatigue and non-fatigue conditions using logistic regression classifiers," *Biomedical Sciences Instrumentation*, vol. 50, pp. 314–321, 2014.
- [63] K. Marri and R. Swaminathan, "Classification of muscle fatigue using surface electromyography signals and multifractals," in *2015 12th International Conference on Fuzzy Systems and Knowledge Discovery (FSKD)*. IEEE, 2015, pp. 669–674.

- [64] P. Karthick, D. M. Ghosh, and S. Ramakrishnan, "Surface electromyography based muscle fatigue detection using high-resolution time-frequency methods and machine learning algorithms," *Computer methods and programs in biomedicine*, vol. 154, pp. 45–56, 2018.
- [65] K. Marri and R. Swaminathan, "Classification of muscle fatigue in dynamic contraction using surface electromyography signals and multifractal singularity spectral analysis," *Journal of Dynamic Systems, Measurement, and Control*, vol. 138, no. 11, p. 111008, 2016.
- [66] P. Karthick, S. Ramakrishnan *et al.*, "Muscle fatigue analysis in isometric contractions using geometric features of surface electromyography signals," *Biomedical Signal Processing and Control*, vol. 68, p. 102603, 2021.
- [67] S. Äyrämö, "Neuromuscular fatigue after short-term maximal run in child, youth, and adult athletes," Master's thesis, 2013.
- [68] R. A. Tibana, J. Prestes, D. da Cunha Nascimento, O. V. Martins, F. S. De Santana, and S. Balsamo, "Higher muscle performance in adolescents compared with adults after a resistance training session with different rest intervals," *The Journal of Strength & Conditioning Research*, vol. 26, no. 4, pp. 1027–1032, 2012.
- [69] Y. Zhang, S. Chen, W. Cao, P. Guo, D. Gao, M. Wang, J. Zhou, and T. Wang, "Mffnet: Multi-dimensional feature fusion network based on attention mechanism for semg analysis to detect muscle fatigue," *Expert Systems with Applications*, vol. 185, p. 115639, 2021.
- [70] D. B. Krishnamani, K. PA, and R. Swaminathan, "Variational mode decomposition based differentiation of fatigue conditions in muscles using surface electromyography signals," *IET Signal Processing*, vol. 14, no. 10, pp. 745–753, 2020.
- [71] J. M. Hart, B. Pietrosimone, J. Hertel, and C. D. Ingersoll, "Quadriceps activation following knee injuries: a systematic review," *Journal of athletic training*, vol. 45, no. 1, pp. 87–97, 2010.
- [72] A. C. Waligora, N. A. Johanson, and B. E. Hirsch, "Clinical anatomy of the quadriceps femoris and extensor apparatus of the knee," *Clinical Orthopaedics and Related Research*, vol. 467, no. 12, pp. 3297–3306, 2009.
- [73] K. Weiss and C. Whatman, "Biomechanics associated with patellofemoral pain and acl injuries in sports," *Sports medicine*, vol. 45, pp. 1325–1337, 2015.
- [74] T. W. Beck, T. J. Housh, A. C. Fry, J. T. Cramer, J. P. Weir, B. K. Schilling, M. J. Falvo, and C. A. Moore, "A wavelet-based analysis of surface mechanomyographic signals from the quadriceps femoris," *Muscle & Nerve: Official Journal of the American Association of Electrodiagnostic Medicine*, vol. 39, no. 3, pp. 355–363, 2009.

- [75] K. T. Ebersole and D. M. Malek, "Fatigue and the electromechanical efficiency of the vastus medialis and vastus lateralis muscles," *Journal of athletic training*, vol. 43, no. 2, pp. 152–156, 2008.
- [76] M. Grabiner, T. Koh, and G. Miller, "Fatigue rates of vastus medialis oblique and vastus lateralis during static and dynamic knee extension," *Journal of orthopaedic research*, vol. 9, no. 3, pp. 391–397, 1991.
- [77] H. J. Hermens, B. Freriks, R. Merletti, D. Stegeman, J. Blok, G. Rau, C. Disselhorst-Klug, and G. Hägg, "European recommendations for surface electromyography," *Roessingh research and development*, vol. 8, no. 2, pp. 13–54, 1999.
- [78] A. Rainoldi, G. Melchiorri, and I. Caruso, "A method for positioning electrodes during surface emg recordings in lower limb muscles," *Journal of neuroscience methods*, vol. 134, no. 1, pp. 37–43, 2004.
- [79] A.-K. Stensdotter, P. Hodges, R. Mellor, G. Sundelin, and C. Häger-Ross, "Quadriceps activation in closed and in open kinetic chain exercise." *Medicine & Science in Sports & Exercise*, vol. 35, no. 12, pp. 2043–2047, 2003.
- [80] D. Stegeman and H. Hermens, "Standards for surface electromyography: The european project surface emg for non-invasive assessment of muscles (seniam)," *Enschede: Roessingh Research and Development*, vol. 10, pp. 8–12, 2007.
- [81] R. Merletti and P. Di Torino, "Standards for reporting emg data," *J Electromyogr Kinesiol*, vol. 9, no. 1, pp. 3–4, 1999.
- [82] M. Elshafei and E. Shihab, "Towards detecting biceps muscle fatigue in gym activity using wearables," *Sensors*, vol. 21, no. 3, p. 759, 2021.
- [83] B. V. Tamani, "Adquisición de datos usando matlab," *Electrónica-UNMSM*, no. 18, pp. 21–28, 2006.
- [84] A. Phinyomark, A. Nuidod, P. Phukpattaranont, and C. Limsakul, "Feature extraction and reduction of wavelet transform coefficients for emg pattern classification," *Elektronika ir Elektrotechnika*, vol. 122, no. 6, pp. 27–32, 2012.
- [85] M. Nachtgeael, D. Van der Weken, E. E. Kerre, and W. Philips, "Soft computing in image processing: Recent advances," 2007.
- [86] O. J. O. Rodríguez and D. A. S. Bueno, "Determinación de los parámetros asociados al filtro wavelet por umbralización aplicado a filtrado de interferencias electrocardiográficas," *Revista UIS Ingenierías*, vol. 6, no. 2, pp. 33–44, 2007.
- [87] "Calculate channel latencies required for wavelet reconstruction," <https://la.mathworks.com/help/dsp/ug/calculate-the-channel-latencies-required-for-wavelet-reconstruction.html>.
- [88] M. A. Oskoei and H. Hu, "Myoelectric control systems—a survey," *Biomedical signal processing and control*, vol. 2, no. 4, pp. 275–294, 2007.

- [89] O. Wahyunggoro, H. A. Nugroho *et al.*, “Quantitative relationship between feature extraction of semg and upper limb elbow joint angle,” in *2016 International Seminar on Application for Technology of Information and Communication (ISemantic)*. IEEE, 2016, pp. 44–50.
- [90] Z. Qing, Z. Lu, Y. Cai, and J. Wang, “Elements influencing semg-based gesture decoding: muscle fatigue, forearm angle and acquisition time,” *Sensors*, vol. 21, no. 22, p. 7713, 2021.
- [91] S. Thongpanja, A. Phinyomark, P. Phukpattaranont, and C. Limsakul, “Mean and median frequency of emg signal to determine muscle force based on time-dependent power spectrum,” *Elektronika ir Elektrotechnika*, vol. 19, no. 3, pp. 51–56, 2013.
- [92] A. Bawa and K. Banitsas, “Design validation of a low-cost emg sensor compared to a commercial-based system for measuring muscle activity and fatigue,” *Sensors*, vol. 22, no. 15, p. 5799, 2022.
- [93] E. Bisong and E. Bisong, “Google colabatory,” *Building machine learning and deep learning models on google cloud platform: a comprehensive guide for beginners*, pp. 59–64, 2019.
- [94] F. Akram, S. M. Han, and T.-S. Kim, “An efficient word typing p300-bci system using a modified t9 interface and random forest classifier,” *Computers in biology and medicine*, vol. 56, pp. 30–36, 2015.
- [95] X. Wu, V. Kumar, J. Ross Quinlan, J. Ghosh, Q. Yang, H. Motoda, G. J. McLachlan, A. Ng, B. Liu, P. S. Yu *et al.*, “Top 10 algorithms in data mining,” *Knowledge and information systems*, vol. 14, pp. 1–37, 2008.
- [96] S. E. Jero, K. D. Bharathi, P. Karthick, and S. Ramakrishnan, “Muscle fatigue analysis in isometric contractions using geometric features of surface electromyography signals,” *Biomedical Signal Processing and Control*, vol. 68, 2021.
- [97] F. A. Mahdavi, S. A. Ahmad, M. H. Marhaban, and M.-R. Akbarzadeh-T, “Surface electromyography feature extraction based on wavelet transform,” *International Journal of Integrated Engineering*, vol. 4, no. 3, 2012.
- [98] D. K. Kumar, S. P. Arjunan, and G. R. Naik, “Measuring increase in synchronization to identify muscle endurance limit,” *IEEE transactions on neural systems and rehabilitation engineering*, vol. 19, no. 5, pp. 578–587, 2011.
- [99] H. Kim, J. Lee, and J. Kim, “Electromyography-signal-based muscle fatigue assessment for knee rehabilitation monitoring systems,” *Biomedical engineering letters*, vol. 8, pp. 345–353, 2018.
- [100] M. Bilodeau, S. Schindler-Ivens, D. Williams, R. Chandran, and S. Sharma, “Emg frequency content changes with increasing force and during fatigue in the quadriceps femoris muscle of men and women,” *Journal of electromyography and kinesiology*, vol. 13, no. 1, pp. 83–92, 2003.

- [101] A. L. Hicks, J. Kent-Braun, and D. S. Ditor, "Sex differences in human skeletal muscle fatigue," *Exercise and sport sciences reviews*, vol. 29, no. 3, pp. 109–112, 2001.
- [102] S. F. D. Toro, S. Santos-Cuadros, E. Olmeda, C. Álvarez-Caldas, V. Díaz, and J. L. San Román, "Is the use of a low-cost semg sensor valid to measure muscle fatigue?" *Sensors*, vol. 19, no. 14, p. 3204, 2019.
- [103] S. Karheily, A. Moukadem, J.-B. Courbot, and D. O. Abdeslam, "semg time-frequency features for hand movements classification," *Expert Systems with Applications*, vol. 210, p. 118282, 2022.
- [104] J. M. Fajardo, O. Gomez, and F. Prieto, "Emg hand gesture classification using handcrafted and deep features," *Biomedical Signal Processing and Control*, vol. 63, p. 102210, 2021.
- [105] J. H. Viitasalo and P. V. Komi, "Signal characteristics of emg during fatigue," *European journal of applied physiology and occupational physiology*, vol. 37, pp. 111–121, 1977.
- [106] F. B. Stulen and C. J. De Luca, "The relation between the myoelectric signal and physiological properties of constant-force isometric contractions," *Electroencephalography and Clinical Neurophysiology*, vol. 45, no. 6, pp. 681–698, 1978.
- [107] J. V. Basmajian, "Their function revealed by electromyography," *Muscle Alive*, vol. 212, 1985.
- [108] A. Phinyomark, C. Limsakul, and P. Phukpattaranont, "Application of wavelet analysis in emg feature extraction for pattern classification," *Measurement Science Review*, vol. 11, no. 2, pp. 45–52, 2011.
- [109] G. Corvini and S. Conforto, "A simulation study to assess the factors of influence on mean and median frequency of semg signals during muscle fatigue," *Sensors*, vol. 22, no. 17, p. 6360, 2022.
- [110] S. Belkacem, R. E. Bekka, and M. Nouredine, "Influence of mvc on temporal and spectral features of simulated surface electromyographic signals," *Critical ReviewsTM in Biomedical Engineering*, vol. 47, no. 5, 2019.
- [111] M. Papakostas, V. Kanal, M. Abujelala, K. Tsiakas, and F. Makedon, "Physical fatigue detection through emg wearables and subjective user reports: a machine learning approach towards adaptive rehabilitation," in *Proceedings of the 12th ACM international conference on pervasive technologies related to assistive environments*, 2019, pp. 475–481.
- [112] Q. Li and K. Doi, "Analysis and minimization of overtraining effect in rule-based classifiers for computer-aided diagnosis," *Medical physics*, vol. 33, no. 2, pp. 320–328, 2006.

- [113] A. G. Glaros and R. B. Kline, "Understanding the accuracy of tests with cutting scores: The sensitivity, specificity, and predictive value model," *Journal of clinical psychology*, vol. 44, no. 6, pp. 1013–1023, 1988.
- [114] R. Budgett, "Fatigue and underperformance in athletes: the overtraining syndrome." *British journal of sports medicine*, vol. 32, no. 2, pp. 107–110, 1998.
- [115] L. T. MacKinnon, "Overtraining effects on immunity and performance in athletes," *Immunology and cell biology*, vol. 78, no. 5, pp. 502–509, 2000.
- [116] D. K. Schneider, B. Grawe, R. A. Magnussen, A. Ceasar, S. N. Parikh, E. J. Wall, A. J. Colosimo, C. C. Kaeding, and G. D. Myer, "Outcomes after isolated medial patellofemoral ligament reconstruction for the treatment of recurrent lateral patellar dislocations: a systematic review and meta-analysis," *The American journal of sports medicine*, vol. 44, no. 11, pp. 2993–3005, 2016.
- [117] A. Moniri, D. Terracina, J. Rodriguez-Manzano, P. H. Strutton, and P. Georgiou, "Real-time forecasting of semg features for trunk muscle fatigue using machine learning," *IEEE Transactions on Biomedical Engineering*, vol. 68, no. 2, pp. 718–727, 2020.

Appendices

.1 Appendix 1.

FORMULARIO DE CONSENTIMIENTO

Yo, [nombre completo del participante], con cédula de identidad [número de cédula], por medio del presente, otorgo mi consentimiento voluntario para participar en el proyecto de investigación titulado: "Análisis de señales sEMG de alta frecuencia" dirigido por Felix Vladimir Bonilla Venegas, docente de la Universidad de Investigación de Tecnología Experimental Yachay.

A continuación, se detallan los términos y condiciones del consentimiento:

Título del Proyecto: Análisis de señales sEMG de alta frecuencia
 Nombre del Investigador Principal: Felix Vladimir Bonilla Venegas
 Correo electrónico: fbonilla@yachaytech.edu.ec

Detalles:

Estoy participando en la construcción de una base de datos de señales electromiográficas de superficie (sEMG). A través de este documento, doy mi consentimiento para que los datos recopilados sean utilizados con fines académicos.

Las señales sEMG serán utilizadas con el fin de realizar un análisis de características para la detección temprana de la fatiga muscular. Además, las señales medidas servirán para contar con una base de datos para en trabajos futuros, dentro del plan de trabajo del presente proyecto de investigación, poder crear una red neuronal que permita la detección automática de la fatiga.

Se garantiza que las señales sEMG no contendrán ninguna referencia que pueda identificarme personalmente. Mi información personal será tratada de forma confidencial y mi nombre será reemplazado por un número.

El responsable de la actividad me proporcionará las indicaciones necesarias para realizar las mediciones de las señales sEMG.

Por favor, marque en todos los cuadros a continuación:

1. Confirmando que he leído y entiendo toda la información indicada anteriormente sobre el estudio.	
2. Entiendo que mi participación es voluntaria y soy libre de retirarme en cualquier momento sin dar ninguna razón.	
3. Entiendo que cuando los resultados de la investigación sean publicados no se usará información personal.	
4. Estoy de acuerdo en participar en el estudio y seguir las instrucciones del instructor.	

Adicionalmente, declaro que he recibido respuestas satisfactorias a todas mis preguntas relacionadas con el proyecto y entiendo plenamente los beneficios asociados con mi participación.

Por medio de mi firma, confirmo que he leído y comprendido los detalles del proyecto mencionados anteriormente, y otorgo mi consentimiento para participar en el estudio "Análisis de señales sEMG de alta frecuencia".

Nombre completo del participante: _____

Firma: _____

Fecha: _____

.2 Appendix 2.

Listing 1: MATLAB Script

```
1 len = length(p1de1);
2 h = 20/(len-1);
3 time = (0:h:20)';
4 plot(time,p1de1);
5
6 % Participant 1
7 s1a1 = [time,p1ae1];
8 s1d1 = [time,p1de1];
9 s1a2 = [time,p1ae2];
10 s1d2 = [time,p1de2];
11
12 % Participant 2
13 s2a1 = [time,p2ae1];
14 s2d1 = [time,p2de1];
15 s2a2 = [time,p2ae2];
16 s2d2 = [time,p2de2];
17
18 % Participant 3
19 s3a1 = [time,p3ae1];
20 s3d1 = [time,p3de1];
21 s3a2 = [time,p3ae2];
22 s3d2 = [time,p3de2];
23
24 % Participant 4
25 s4a1 = [time,p4ae1];
26 s4d1 = [time,p4de1];
27 s4a2 = [time,p4ae2];
28 s4d2 = [time,p4de2];
29
30 % Participant 5
31 s5a1 = [time,p5ae1];
32 s5d1 = [time,p5de1];
33 s5a2 = [time,p5ae2];
34 s5d2 = [time,p5de2];
35
36 % Participant 6
37 s6a1 = [time,p6ae1];
38 s6d1 = [time,p6de1];
39 s6a2 = [time,p6ae2];
40 s6d2 = [time,p6de2];
```

```
41
42 % Participant 7
43 s7a1 = [time,p7ae1];
44 s7d1 = [time,p7de1];
45 s7a2 = [time,p7ae2];
46 s7d2 = [time,p7de2];
47
48 % Participant 8
49 s8a1 = [time,p8ae1];
50 s8d1 = [time,p8de1];
51 s8a2 = [time,p8ae2];
52 s8d2 = [time,p8de2];
53
54 % Participant 9
55 s9a1 = [time,p9ae1];
56 s9d1 = [time,p9de1];
57 s9a2 = [time,p9ae2];
58 s9d2 = [time,p9de2];
59
60 % Participant 10
61 s10a1 = [time,p10ae1];
62 s10d1 = [time,p10de1];
63 s10a2 = [time,p10ae2];
64 s10d2 = [time,p10de2];
```

.3 Appendix 3.

Listing 2: Random Forest Script

```
1 import pandas as pd
2 from sklearn.model_selection import train_test_split
3 from sklearn.ensemble import RandomForestClassifier
4 from sklearn.metrics import accuracy_score
5 from sklearn.metrics import confusion_matrix
6
7 # Load training and test data
8 dataX = pd.read_excel('/content/data-train.xlsx')
9 dataY = pd.read_excel('/content/data-test.xlsx')
10
11 X_train = dataX[['MAV', 'RMS', 'MNF']]
12 X_test = dataY[['MAV', 'RMS', 'MNF']]
13
14 y_train = dataX[['Classification']]
15 y_test = dataY[['Classification']]
16
17 # Initializing the Random Forest classifier
18 rf_classifier = RandomForestClassifier(n_estimators=100, random_state
    =41)
19
20 # Training the model
21 rf_classifier.fit(X_train, y_train)
22
23 # Predicting labels for the test set
24 y_pred = rf_classifier.predict(X_test)
25
26 # Calculate the accuracy of the model.
27 accuracy = accuracy_score(y_test, y_pred)
28 print("Precisi n del modelo: {:.2f}%".format(accuracy * 100))
29
30 # Calculate the confusion matrix
31 conf_matrix = confusion_matrix(y_test, y_pred)
32 print(conf_matrix)
33
34 # Extract the values of the confusion matrix
35 TN, FP, FN, TP = conf_matrix.ravel()
36
37 # Calculate sensitivity and specificity
38 sensitivity = TP / (TP + FN)
39 specificity = TN / (TN + FP)
```

40

```
41 print("Sensibilidad del modelo Ramdom Forest: {:.2f}%".format(  
    sensitivity * 100))  
42 print("Especificidad del modelo Ramdom Forest: {:.2f}%".format(  
    specificity * 100))
```

.4 Appendix 4.

Listing 3: Support Vector Machine Script

```
1 from sklearn.svm import SVC
2
3 # Load training and test data
4 dataX = pd.read_excel('/content/data-train.xlsx')
5 dataY = pd.read_excel('/content/data-test.xlsx')
6
7 X_train = dataX[['MAV', 'RMS', 'MNF']]
8 X_test = dataY[['MAV', 'RMS', 'MNF']]
9
10 y_train = dataX[['Classification']]
11 y_test = dataY[['Classification']]
12
13 # Initializing the SVM classifier
14 svm_classifier = SVC(kernel='rbf', random_state=41)
15
16 # Training the SVM model
17 svm_classifier.fit(X_train, y_train)
18
19 # Predicting the labels for the test set using SVM
20 y_pred_svm = svm_classifier.predict(X_test)
21
22 # Calculate the accuracy of the SVM model
23 accuracy_svm = accuracy_score(y_test, y_pred_svm)
24 print("Precisi n del modelo SVM: {:.2f}%".format(accuracy_svm * 100))
25
26 # Calculate the confusion matrix
27 conf_matrix = confusion_matrix(y_test, y_pred)
28 print(conf_matrix)
29
30 # Extract the values of the confusion matrix
31 TN, FP, FN, TP = conf_matrix.ravel()
32
33 # Calculate sensitivity and specificity
34 sensitivity = TP / (TP + FN)
35 specificity = TN / (TN + FP)
36
37 print("Sensibilidad del modelo SVM: {:.2f}%".format(sensitivity * 100)
38       )
38 print("Especificidad del modelo SVM: {:.2f}%".format(specificity *
39       100))
```

.5 Appendix 5.

Listing 4: K-Nearest Neighbor Script

```
1 from sklearn.neighbors import KNeighborsClassifier
2
3 # Load training and test data
4 dataX = pd.read_excel('/content/data-train.xlsx')
5 dataY = pd.read_excel('/content/data-test.xlsx')
6
7 X_train = dataX[['MAV', 'RMS', 'MNF']]
8 X_test = dataY[['MAV', 'RMS', 'MNF']]
9
10 y_train = dataX[['Classification']]
11 y_test = dataY[['Classification']]
12
13 # Inicializar el clasificador KNN con un valor de k arbitrario (por
    ejemplo, k=5)
14 knn_classifier = KNeighborsClassifier(n_neighbors=2)
15
16 # Entrenar el modelo KNN
17 knn_classifier.fit(X_train, y_train)
18
19 # Predecir las etiquetas para el conjunto de prueba usando KNN
20 y_pred_knn = knn_classifier.predict(X_test)
21
22 # Calcular la precisi n del modelo KNN
23 accuracy_knn = accuracy_score(y_test, y_pred_knn)
24 print("Precisi n del modelo KNN: {:.2f}%".format(accuracy_knn * 100))
25
26 # Calculate the confusion matrix
27 conf_matrix = confusion_matrix(y_test, y_pred)
28 print(conf_matrix)
29
30 # Extract the values of the confusion matrix
31 TN, FP, FN, TP = conf_matrix.ravel()
32
33 # Calculate sensitivity and specificity
34 sensitivity = TP / (TP + FN)
35 specificity = TN / (TN + FP)
36
37 print("Sensibilidad del modelo KNN: {:.2f}%".format(sensitivity * 100)
    )
38 print("Especificidad del modelo KNN: {:.2f}%".format(specificity * 100)
    )
```


100))
